Linear Algebra and its Applications 654 (2022) 177–209

Contents lists available at ScienceDirect

Linear Algebra and its Applications

www.elsevier.com/locate/laa

Two complementary block Macaulay matrix algorithms to solve multiparameter eigenvalue problems ☆

Christof Vermeersch *, Bart De Moor

Center for Dynamical Systems, Signal Processing, and Data Analytics (STADIUS), Department of Electrical Engineering (ESAT), KU Leuven, Kasteelpark Arenberg 10, 3001 Leuven, Belgium

ARTICLE INFO

Article history:
Received 23 June 2021
Accepted 12 August 2022
Available online 6 September 2022
Submitted by V. Mehrmann

MSC:
15A18
15A22
15B05
93B15

Keywords:
Multiparameter eigenvalue problems
Matrix pencils
Block Macaulay matrix
Realization theory

ABSTRACT

We consider two algorithms that use the block Macaulay matrix to solve (rectangular) multiparameter eigenvalue problems (MEPs). On the one hand, a multidimensional realization problem in the null space of the block Macaulay matrix constructed from the coefficient matrices of an MEP results in a standard eigenvalue problem (SEP), the eigenvalues and eigenvectors of which yield the solutions of that MEP. On the other hand, we propose a complementary algorithm to solve MEPs that considers the data in the column space of the sparse and structured block Macaulay matrix directly, avoiding the computation of a numerical basis matrix of the null space. This paper generalizes, in a certain sense, traditional Macaulay matrix techniques from multivariate polynomial system solving to the block Macaulay matrix in the MEP setting.

☆ This work was supported in part by the KU Leuven: Research Fund (projects C16/15/059, C3/19/053, C24/18/022, and C3/20/117), Industrial Research Fund (fellowships 13-0260, IOFm/16/004, and IOFm/20/002), and several Leuven Research & Development projects, in part by Flemish Government agencies: FWO (EOS project G0F6718N, SBO project S005319, infrastructure project I013218N, and TBM project T001919N), EWI (Flanders AI Research Program VR-21-29.01-0077), and VLAIO (City of Things COT.2018.018, Baekeland PhD mandate HBC.2019.2204, and innovation mandate HBC.2019.2209), and in part by the European Commission (ERC Adv. Grant under grant 885682). The work of Christof Vermeersch was supported by the FWO Strategic Basic Research fellowship under grant SB/1SA1319N.

* Corresponding author.
E-mail addresses: christof.vermeersch@esat.kuleuven.be (C. Vermeersch), bart.demoor@esat.kuleuven.be (B. De Moor).

https://doi.org/10.1016/j.laa.2022.08.014

1. Introduction

Many natural and scientific phenomena exhibit intrinsic system dynamics that can be captured in a standard eigenvalue problem (SEP). The eigenvalues and eigenvectors that correspond to those phenomena describe the proper (the prefix *eigen-* is adopted from the German word *eigen*, which means *proper* and was presumably first coined by Hilbert [29]) evolution of the system dynamics along the eigenvector directions. For some phenomena, however, a single spectral parameter does not capture the system dynamics entirely and multiple spectral parameters, or eigentuples of eigenvalues, come into the picture, for instance in partial differential equations. Historically, multiparameter spectral theory has its roots in the classical problem of solving boundary-value problems for partial differential equations by the method of separation of variables [3,43,47]. For example, the vibration problem of an elliptic membrane in two ellipsoidal coordinates, i.e., the two-dimensional Helmholtz equation, leads to the study of a pair of ordinary differential equations, both of which share two spectral parameters. This corresponds to a two-parameter eigenvalue problem [43,47]. The presence of multiple spectral parameters (eigentuples instead of eigenvalues) links the evolution of the different ordinary differential equations obtained from the separation of variables in an elementary fashion. Recently, we have shown that the least-squares identification of linear time-invariant systems is, in essence, also a (rectangular) multiparameter eigenvalue problem [20,21,50]. Despite their applicability and natural relation to SEPs, multiparameter eigenvalue problems (MEPs) have not yet been widely diffused among the general scientific community. The literature about solving one-parameter eigenvalue problems, i.e., SEPs, GEPs (generalized eigenvalue problems), and PEPs (polynomial eigenvalue problems), is vast and mature. PEPs are usually linearized into larger GEPs [28,49] and the resulting matrix pencils are solved via one of the many available, efficient SEP or GEP solvers. Techniques to solve MEPs, on the contrary, have been explored much less. We make a distinction between algorithms to solve square MEPs and algorithms to solve rectangular MEPs, although both problems are related.

Classical *square* MEPs, on the one hand, are typically solved via simultaneous triangularization of the associated coupled GEPs [30,35,42,48]. This approach works for any number of spectral parameters and retrieves all the solutions, but is limited by the size of the coupled GEPs. Also iterative nonlinear optimization algorithms can be used to retrieve one (or some) of the solutions, e.g., gradient descent techniques [8,9,12], minimal residual quotient iterations [7], or Newton-based methods [10], but these optimization approaches are heuristic (they depend on an initial guess) and result in numerical approx-

imations of the eigentuples and eigenvectors. In the last two decades, a renewed interest in the topic has led to several efficient homotopy continuation algorithms [22,41,44] and subspace approaches [30,31,33,34,45] to overcome scalability and convergence issues. These algorithms can also solve polynomial square MEPs, either directly or after a linearization step [32,44].

In our earlier work [20,21,50], on the other hand, we have introduced the block Macaulay matrix, which allows us to solve *rectangular* MEPs via a multidimensional realization problem in the null space of that matrix. We consider in this paper the complementarity between the null space and column space of the block Macaulay matrix in order to develop a new, complementarity algorithm that works on the data in the columns directly. This observation stems from a similar complementarity in multivariate polynomial system solving, in which the null space and column space of the traditional Macaulay matrix both give rise to a root-finding algorithm [51]. We use well-established tools from numerical linear algebra, such as the singular value decomposition or QR-decomposition, to solve rectangular MEPs (which are essentially disguised systems of multivariate polynomial equations with some variables that only appear "linearly"). In contrast to the classical MEPs with square coefficient matrices, we consider in our research rectangular MEPs, which arise, for example, in system identification problems [20,21,50] or multiparameter generalizations of the Heine–Stieltjes spectral problem [46]. We can even transform quite a few classical square MEPs into equivalent rectangular MEPs (see Section 2). In that sense, the two block Macaulay matrix algorithms of this paper also supplement the set of existing algorithms to solve classical square problems.

Outline and main contributions The remainder of this paper proceeds as follows: Section 2 defines the rectangular MEP and Section 3 introduces the block Macaulay matrix, which is constructed from the coefficient matrices of a rectangular MEP. The (right) null space of this block Macaulay matrix has a special (backward block multi-)shift-invariant structure, which allows us to find the eigentuples and eigenvectors of the rectangular MEP via a multidimensional realization problem in that null space. We revisit this existing null space based algorithm to solve rectangular MEPs in Section 4. Our **main contributions** are (i) the observation that the complementarity between the null space and column space of the block Macaulay matrix results in an equivalent multidimensional realization problem in the column space and (ii) a second block Macaulay matrix algorithm to solve polynomial rectangular MEPs, using only numerical linear algebra "work horses" like the singular value decomposition and QR-decomposition. We develop this column space based algorithm in Section 5. Several numerical examples illustrate both algorithms in Section 6. Finally, we summarize this paper and point at ideas for future research in Section 7. Appendix A covers the structure of backward scalar/block single/multi-shift-invariant finite dimensional subspaces, like the affine part of the null space of the block Macaulay matrix, in more depth.

Notation We denote scalars by lowercase letters, e.g., a, and tuples/vectors by boldface lowercase letters, e.g., $\boldsymbol{a}$. Matrices are characterized by boldface uppercase letters, e.g., $\boldsymbol{A}$. When a matrix contains one or more parameters, for example, the combined coefficient matrix of an MEP, we use a bold calligraphic font, e.g., $\boldsymbol{\mathcal{A}}(\boldsymbol{a})$ with parameter $\boldsymbol{a}$. We use a subscript to indicate an element or submatrix of a tuple/vector or matrix, e.g., a_1 is the first element of the vector $\boldsymbol{a}$.

2. Multiparameter eigenvalue problems

Multiparameter eigenvalue problems (MEPs) naturally extend the typical structure of standard eigenvalue problems and involve eigentuples $\boldsymbol{\lambda} = (\lambda_1, \ldots, \lambda_n)$ of eigenvalues instead of single eigenvalues λ. Several manifestations of MEPs appear in the literature, e.g., the classical square problems by Atkinson [1], Carmichael [13,14,15], Plestenjak et al. [43], Volkmer [52] and the rectangular problems in this paper and by Shapiro and Shapiro [46], De Moor [21], Vermeersch and De Moor [50]. Therefore, we start by defining the (rectangular[1]) MEP within our block Macaulay matrix framework.

For example, $\left(\boldsymbol{A}_{000} + \boldsymbol{A}_{100}\lambda_1 + \boldsymbol{A}_{025}\lambda_2^2\lambda_3^5\right)\boldsymbol{z} = \boldsymbol{0}$ contains $n = 3$ spectral parameters, combined in eigentuples $(\lambda_1, \lambda_2, \lambda_3)$ with corresponding eigenvectors $\boldsymbol{z}$, and three coefficient matrices $\boldsymbol{A}_{\boldsymbol{\omega}}$. The integer multi-index $\boldsymbol{\omega} = (\omega_1, \ldots, \omega_n) \in \mathbb{N}^n$ labels the powers of the eigenvalues in the monomial $\boldsymbol{\lambda}^{\boldsymbol{\omega}} = \prod_{i=1}^{n} \lambda_i^{\omega_i} = \lambda_1^{\omega_1} \cdots \lambda_n^{\omega_n}$ and indexes the associated coefficient matrices $\boldsymbol{A}_{\boldsymbol{\omega}} = \boldsymbol{A}_{(\omega_1,\ldots,\omega_n)}$. The total degree of a monomial is equal to the sum of its powers, denoted by $|\boldsymbol{\omega}| = \sum_{i=1}^{n} \omega_i$, and the highest total degree of all the monomials determines the degree d_{S} of the MEP. Hence, an integer multi-index $\boldsymbol{\omega} = (0, 2, 5)$ labels the monomial $\lambda_2^2\lambda_3^5$ (with total degree 7) and indexes the associated coefficient matrix $\boldsymbol{A}_{025}$. To keep the notation unambiguous, we use the degree negative lexicographic ordering to order different (multivariate) monomials [5,17]. However, the remainder of this paper remains valid for any graded multivariate monomial ordering.

Definition 1 ***(Degree negative lexicographic ordering)***. If we consider two n-tuples $\boldsymbol{\alpha}, \boldsymbol{\beta} \in \mathbb{N}^n$ and $|\boldsymbol{\alpha}| < |\boldsymbol{\beta}|$ or $|\boldsymbol{\alpha}| = |\boldsymbol{\beta}|$ where in the element-wise difference $\boldsymbol{\beta} - \boldsymbol{\alpha} \in \mathbb{Z}^n$ the left-most non-zero element of the tuple is negative, then two monomials are ordered $\boldsymbol{\lambda}^{\boldsymbol{\alpha}} < \boldsymbol{\lambda}^{\boldsymbol{\beta}}$ by the **degree negative lexicographic ordering**.

Example 1. The degree negative lexicographic ordering orders the monomials in $n = 3$ variables as

$$1 < \lambda_1 < \lambda_2 < \lambda_3 < \lambda_1^2 < \lambda_1\lambda_2 < \lambda_1\lambda_3 < \lambda_2^2 < \lambda_2\lambda_3 < \lambda_3^2 < \lambda_1^3 < \lambda_1^2\lambda_2 < \ldots$$

[1] In the remainder of this paper, we no longer mention the qualification *rectangular* explicitly. We always consider rectangular problems, except when denoted otherwise (for example, during the comparison with classical square problems).

Table 1
Within our block Macaulay matrix framework, we observe four different types of MEPs, organized according to the structure of the monomials in the combined coefficient matrix $\boldsymbol{\mathcal{M}}(\lambda_1, \ldots, \lambda_n)$.

Spectral parameter(s)	Linear	Polynomial
Eigenvalues ($n = 1$)	Type I $\{1, \lambda\}$ SEP/GEP	Type II λ^{ω} PEP
Eigentuples ($n > 1$) ($i = 1, \ldots, n$)	Type III λ_i linear MEP	Type IV $\prod_{i=1}^{n} \lambda_i^{\omega_i}$ polynomial MEP

Definition 2 ***(Multiparameter eigenvalue problem).*** Given coefficient matrices $\boldsymbol{A_\omega} \in \mathbb{R}^{k \times l}$ (with $k \geq l + n - 1$), the **multiparameter eigenvalue problem** $\boldsymbol{\mathcal{M}}(\lambda_1, \ldots, \lambda_n)\, \boldsymbol{z} = \boldsymbol{0}$ consists in finding all n-tuples $\boldsymbol{\lambda} = (\lambda_1, \ldots, \lambda_n) \in \mathbb{C}^n$ and corresponding vectors $\boldsymbol{z} \in \mathbb{C}^{l \times 1} \setminus \{\boldsymbol{0}\}$, so that

$$\boldsymbol{\mathcal{M}}(\lambda_1, \ldots, \lambda_n)\, \boldsymbol{z} = \left(\sum_{\{\boldsymbol{\omega}\}} \boldsymbol{A_\omega} \boldsymbol{\lambda}^{\boldsymbol{\omega}} \right) \boldsymbol{z} = \boldsymbol{0}, \tag{1}$$

where the summation runs over all the multi-indices $\boldsymbol{\omega}$ of the monomials $\boldsymbol{\lambda}^{\boldsymbol{\omega}} = \prod_{i=1}^{n} \lambda_i^{\omega_i}$ and coefficient matrices $\boldsymbol{A_\omega} = \boldsymbol{A}_{(\omega_1, \ldots, \omega_n)}$. The n-tuples $\boldsymbol{\lambda} = (\lambda_1, \ldots, \lambda_n)$ and (non-zero) vectors $\boldsymbol{z}$ are the eigentuples (with eigenvalues $\lambda_1, \ldots, \lambda_n$) and eigenvectors of the MEP, respectively.

The size condition on the coefficient matrices is a necessary (but not a sufficient) condition in order to have zero-dimensional solution set: there are k equations and 1 non-triviality constraint on $\boldsymbol{z}$ (e.g., $\|\boldsymbol{z}\|_2 = 1$) in $l + n$ unknowns (l elements in the eigenvectors and n eigenvalues), thus $k + 1 \geq l + n$. The matrix $\boldsymbol{\mathcal{M}}(\lambda_1, \ldots, \lambda_n)$ is the combined coefficient matrix of the MEP and is a multivariate polynomial in the eigenvalues $\lambda_1, \ldots, \lambda_n$ with matrix coefficients $\boldsymbol{A_\omega}$. Table 1 summarizes the different types of problems that we cover with Definition 2, organized according to the structure of the monomials in $\boldsymbol{\mathcal{M}}(\lambda_1, \ldots, \lambda_n)$, i.e., single eigenvalues versus eigentuples and linear appearance versus polynomial appearance. Examples 2, 3, 4, and 5 (below) each illustrate one of the four types of MEPs. The block Macaulay matrix algorithms in this paper provide an elegant, unifying approach to solve all the problems in Table 1.

Example 2 ***(Type I – SEP/GEP).*** The standard eigenvalue problem (SEP) $\boldsymbol{A}_0 \boldsymbol{z} = \boldsymbol{z}\lambda$, or $(\boldsymbol{A}_0 - \boldsymbol{I}\lambda)\, \boldsymbol{z} = \boldsymbol{0}$, and the generalized eigenvalue problem (GEP) $\boldsymbol{A}_0 \boldsymbol{z} = \boldsymbol{A}_1 \boldsymbol{z}\lambda$, or $(\boldsymbol{A}_0 - \boldsymbol{A}_1 \lambda)\, \boldsymbol{z} = 0$, are MEPs with $n = 1$.

Example 3 ***(Type II – PEP).*** Polynomial eigenvalue problems (PEPs) of degree d_{S} also fit perfectly in Definition 2, with $n = 1$, as

$$\left(\sum_{\{\omega\}} \boldsymbol{A}_\omega \lambda^\omega\right) \boldsymbol{z} = \left(\sum_{i=0}^{d_\mathrm{S}} \boldsymbol{A}_i \lambda^i\right) \boldsymbol{z} = \boldsymbol{0}.$$

For example, a PEP of degree $d_\mathrm{S} = 4$ has five coefficient matrices $\boldsymbol{A}_i \in \mathbb{R}^{k\times l}$ $(k \geq l)$ and is given by

$$\left(\boldsymbol{A}_0 + \boldsymbol{A}_1\lambda + \boldsymbol{A}_2\lambda^2 + \boldsymbol{A}_3\lambda^3 + \boldsymbol{A}_4\lambda^4\right) \boldsymbol{z} = \boldsymbol{0}.$$

Example 4 *(**Type III** – **linear MEP**).* Often, the eigenvalues appear "linearly" in the monomials of the MEP, for example, a linear two-parameter eigenvalue problem (linear 2-EP)

$$\left(\boldsymbol{A}_{00} + \boldsymbol{A}_{10}\lambda_1 + \boldsymbol{A}_{01}\lambda_2\right) \boldsymbol{z} = \boldsymbol{0},$$

with three coefficient matrices $\boldsymbol{A}_{\boldsymbol{\omega}} \in \mathbb{R}^{3\times 2}$,

$$\boldsymbol{A}_{00} = \begin{bmatrix} 2 & 6 \\ 4 & 5 \\ 0 & 1 \end{bmatrix}, \boldsymbol{A}_{10} = \begin{bmatrix} 1 & 0 \\ 0 & 1 \\ 1 & 1 \end{bmatrix}, \text{ and } \boldsymbol{A}_{01} = \begin{bmatrix} 4 & 2 \\ 0 & 8 \\ 1 & 1 \end{bmatrix}.$$

Example 5 *(**Type IV** – **polynomial MEP**).* As a final example, we consider a (multivariate) polynomial MEP of degree $d_\mathrm{S} = 2$ with two parameters and four monomials,

$$\left(\boldsymbol{A}_{00} + \boldsymbol{A}_{10}\lambda_1 + \boldsymbol{A}_{11}\lambda_1\lambda_2 + \boldsymbol{A}_{02}\lambda_2^2\right) \boldsymbol{z} = \boldsymbol{0},$$

which has four coefficient matrices $\boldsymbol{A}_{\boldsymbol{\omega}} \in \mathbb{R}^{3\times 2}$,

$$\boldsymbol{A}_{00} = \begin{bmatrix} 1 & 2 \\ 3 & 4 \\ 3 & 4 \end{bmatrix}, \boldsymbol{A}_{10} = \begin{bmatrix} 2 & 1 \\ 0 & 1 \\ 1 & 3 \end{bmatrix}, \boldsymbol{A}_{11} = \begin{bmatrix} 3 & 4 \\ 2 & 1 \\ 0 & 1 \end{bmatrix}, \text{ and } \boldsymbol{A}_{02} = \begin{bmatrix} 1 & 2 \\ 4 & 2 \\ 2 & 1 \end{bmatrix}.$$

Link between the square and rectangular MEP In the literature, one often encounters the classical square MEP, in which n matrix equations with square coefficient matrices are combined into a multiparameter system [2,41,52]. A linear 2-EP in this classical form is written as

$$\begin{cases} \boldsymbol{\mathcal{W}}_1\left(\lambda_1, \lambda_2\right) \boldsymbol{x} = \left(\boldsymbol{A}_1 + \boldsymbol{B}_1\lambda_1 + \boldsymbol{C}_1\lambda_2\right) \boldsymbol{x} = \boldsymbol{0} \\ \boldsymbol{\mathcal{W}}_2\left(\lambda_1, \lambda_2\right) \boldsymbol{y} = \left(\boldsymbol{A}_2 + \boldsymbol{B}_2\lambda_1 + \boldsymbol{C}_2\lambda_2\right) \boldsymbol{y} = \boldsymbol{0} \end{cases}, \tag{2}$$

where (λ_1, λ_2) are the eigentuples and the tensor products $\boldsymbol{z} = \boldsymbol{x} \otimes \boldsymbol{y} = \mathrm{vec}\left(\boldsymbol{y}\boldsymbol{x}^\mathrm{T}\right)$, with $\|\boldsymbol{x}\|_2 = 1$ and $\|\boldsymbol{y}\|_2 = 1$, are defined as the corresponding eigenvectors.[2] The coefficient

[2] The vectorization $\mathrm{vec}(\cdot)$ is a linear transformation that converts a matrix into a column vector, by stacking the columns of the matrix on top of one another.

matrices $\boldsymbol{A}_1$, $\boldsymbol{A}_2$, $\boldsymbol{B}_1$, $\boldsymbol{B}_2$, $\boldsymbol{C}_1$, and $\boldsymbol{C}_2$ are square matrices. Square linear 2-EPs that are regular (i.e., $\boldsymbol{\Delta}_0 = \boldsymbol{B}_1 \otimes \boldsymbol{C}_2 - \boldsymbol{C}_1 \otimes \boldsymbol{B}_2$ is a non-singular matrix) can be transformed into an equivalent rectangular linear 2-EP via Kronecker products, as the next example illustrates.

Example 6. On the first page of his book, Volkmer [52] used the following problem to introduce several aspects of multiparameter spectral theory (a classical square linear 2-EP as in (2)):

$$\boldsymbol{A}_1 = \begin{bmatrix} 4 & 0 & 0 \\ 0 & 0 & 0 \\ 0 & 0 & 0 \end{bmatrix}, \boldsymbol{B}_1 = \begin{bmatrix} 1 & 0 & 0 \\ 0 & 6 & 0 \\ 0 & 0 & 1 \end{bmatrix}, \boldsymbol{C}_1 = \begin{bmatrix} 0 & 1 & 0 \\ 1 & 0 & 1 \\ 0 & 1 & 0 \end{bmatrix},$$
$$\boldsymbol{A}_2 = \begin{bmatrix} 20 & 0 \\ 0 & 0 \end{bmatrix}, \boldsymbol{B}_2 = \begin{bmatrix} 0 & \sqrt{3} \\ \sqrt{3} & 0 \end{bmatrix}, \text{ and } \boldsymbol{C}_2 = \begin{bmatrix} 7 & 0 \\ 0 & 1 \end{bmatrix}.$$

As shown by Atkinson [1], this regular linear square 2-EP is equivalent with the coupled GEPs

$$\begin{cases} \boldsymbol{\Delta}_1 \boldsymbol{z} = \boldsymbol{\Delta}_0 \lambda_1 \boldsymbol{z} \\ \boldsymbol{\Delta}_2 \boldsymbol{z} = \boldsymbol{\Delta}_0 \lambda_2 \boldsymbol{z} \end{cases}, \tag{3}$$

with $\|\boldsymbol{z}\|_2 = 1$, $\boldsymbol{\Delta}_0 = \boldsymbol{B}_1 \otimes \boldsymbol{C}_2 - \boldsymbol{C}_1 \otimes \boldsymbol{B}_2$, $\boldsymbol{\Delta}_1 = \boldsymbol{A}_1 \otimes \boldsymbol{C}_2 - \boldsymbol{C}_1 \otimes \boldsymbol{A}_2$, and $\boldsymbol{\Delta}_2 = \boldsymbol{B}_1 \otimes \boldsymbol{A}_2 - \boldsymbol{A}_1 \otimes \boldsymbol{B}_2$ ($\boldsymbol{\Delta}_i \in \mathbb{R}^{6\times 6}$). Via these equivalent coupled GEPs, we can transform the linear square 2-EP into its equivalent rectangular form:

$$\left(\begin{bmatrix} \boldsymbol{\Delta}_1 \\ \boldsymbol{\Delta}_2 \end{bmatrix} - \begin{bmatrix} \boldsymbol{\Delta}_0 \\ 0 \end{bmatrix} \lambda_1 - \begin{bmatrix} 0 \\ \boldsymbol{\Delta}_0 \end{bmatrix} \lambda_2 \right) \boldsymbol{z} = \boldsymbol{0}. \tag{4}$$

Note that this transformation leads to a linear rectangular MEP where the number of rows k is strictly larger than the necessary $l + n - 1$. The two block Macaulay matrix algorithms that we present in this paper can also be used to solve this type of problems. Since the Kronecker products typically result in large coefficient matrices, this approach should only be applied to small problems. Furthermore, we need to be careful in the case of singular problems (i.e., $\boldsymbol{\Delta}_0$ is a singular matrix), where the equivalence between the square problem and the coupled GEPs is not straightforward, as discussed by Košir and Plestenjak [36], Muhič and Plestenjak [40]. We do not elaborate any further on this connection.

3. Block Macaulay matrix

In earlier work [20,21,50], we have introduced the block Macaulay matrix in order to solve MEPs that arrive in the context of system identification. It is a block matrix extension of the traditional Macaulay matrix [37,38], a sparse and structured matrix primarily used to solve systems of multivariate polynomial equations [4–6,23–25,51].

The MEP $\boldsymbol{\mathcal{M}}(\lambda_1, \ldots, \lambda_n)\, \boldsymbol{z} = \boldsymbol{0}$ in (1) constitutes the so-called *seed equation* and its corresponding block Macaulay matrix is obtained via block forward multi-shift recursions (block FmSRs): we generate "new" matrix equations $\left\{\prod_{i=1}^{n} \lambda_i^{d_i}\right\} \boldsymbol{\mathcal{M}}(\lambda_1, \ldots, \lambda_n)\, \boldsymbol{z} = \boldsymbol{0}$ by multiplying the seed equation (i.e., the generating MEP) with different monomials $\prod_{i=1}^{n} \lambda_i^{d_i}$ of increasing total degree $d_{\mathrm{R}} = \sum_{i=1}^{n} d_i$, and we organize the coefficient matrices of these matrix equations as the block rows of the block Macaulay matrix.

Example 7. For example, if we start with a quadratic two-parameter eigenvalue problem (Type IV),

$$\left(\boldsymbol{A}_{00} + \boldsymbol{A}_{10}\lambda_1 + \boldsymbol{A}_{01}\lambda_2 + \boldsymbol{A}_{20}\lambda_1^2 + \boldsymbol{A}_{11}\lambda_1\lambda_2 + \boldsymbol{A}_{02}\lambda_2^2\right) \boldsymbol{z} = \boldsymbol{0},$$

and multiply it by the two eigenvalues λ_1 and λ_2, then we obtain two "new" matrix equations:

$$\begin{aligned}
\lambda_1 \left(\boldsymbol{A}_{00} + \boldsymbol{A}_{10}\lambda_1 + \boldsymbol{A}_{01}\lambda_2 + \boldsymbol{A}_{20}\lambda_1^2 + \boldsymbol{A}_{11}\lambda_1\lambda_2 + \boldsymbol{A}_{02}\lambda_2^2\right) \boldsymbol{z} &= \boldsymbol{0} \\
\lambda_2 \left(\boldsymbol{A}_{00} + \boldsymbol{A}_{10}\lambda_1 + \boldsymbol{A}_{01}\lambda_2 + \boldsymbol{A}_{20}\lambda_1^2 + \boldsymbol{A}_{11}\lambda_1\lambda_2 + \boldsymbol{A}_{02}\lambda_2^2\right) \boldsymbol{z} &= \boldsymbol{0}.
\end{aligned}$$

We can continue this process with monomials of increasing total degree d_{R}, i.e.,

$$\underbrace{\lambda_1, \lambda_2}_{d_{\mathrm{R}}=1}, \underbrace{\lambda_1^2, \lambda_1\lambda_2, \lambda_2^2}_{d_{\mathrm{R}}=2}, \underbrace{\lambda_1^3, \lambda_1^2\lambda_2, \ldots}_{d_{\mathrm{R}}\geq 3}$$

and arrange the resulting coefficient matrices in a block Macaulay matrix (seed equation in red):

$$\begin{array}{c} \\ 1 \\ \lambda_1 \\ \lambda_2 \\ \lambda_1^2 \\ \\ \end{array}
\begin{array}{c}
\begin{array}{ccccccc} \boldsymbol{z} & \lambda_1\boldsymbol{z} & \lambda_2\boldsymbol{z} & \lambda_1^2\boldsymbol{z} & \lambda_1\lambda_2\boldsymbol{z} & \lambda_2^2\boldsymbol{z} & \lambda_1^3\boldsymbol{z} \end{array} \\
\left[\begin{array}{c|c|c|c|c|c|c|c}
\boldsymbol{A}_{00} & \boldsymbol{A}_{10} & \boldsymbol{A}_{01} & \boldsymbol{A}_{20} & \boldsymbol{A}_{11} & \boldsymbol{A}_{02} & \boldsymbol{0} & \cdots \\
\boldsymbol{0} & \boldsymbol{A}_{00} & \boldsymbol{0} & \boldsymbol{A}_{10} & \boldsymbol{A}_{01} & \boldsymbol{0} & \boldsymbol{A}_{20} & \cdots \\
\boldsymbol{0} & \boldsymbol{0} & \boldsymbol{A}_{00} & \boldsymbol{0} & \boldsymbol{A}_{10} & \boldsymbol{A}_{01} & \boldsymbol{0} & \cdots \\
\boldsymbol{0} & \boldsymbol{0} & \boldsymbol{0} & \boldsymbol{A}_{00} & \boldsymbol{0} & \boldsymbol{0} & \boldsymbol{A}_{10} & \cdots \\
\vdots & \vdots & \vdots & \vdots & \vdots & \vdots & \vdots & \ddots
\end{array}\right]
\end{array}.$$

When we further *enlarge* the block Macaulay matrix via block FmSRs with monomials of increasing total degree d_{R}, we obtain a sparse and structured matrix, as visualized in Fig. 1.

Definition 3 ***(Block Macaulay matrix).*** Given the MEP $\boldsymbol{\mathcal{M}}(\lambda_1, \ldots, \lambda_n)\, \boldsymbol{z} = \boldsymbol{0}$ of degree d_{S}, which serves as the seed equation, the **block Macaulay matrix** $\boldsymbol{M}(d) \in \mathbb{R}^{p(d)\times q(d)}$ of degree d contains the coefficient matrices of the seed equation and the matrix equations generated by the block FmSRs with monomials of increasing total degree $d_{\mathrm{R}} = 1, \ldots, (d - d_{\mathrm{S}})$, i.e.,

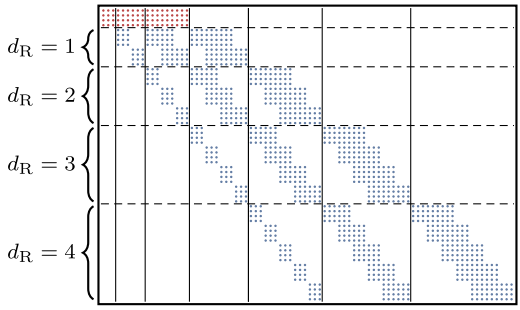

Fig. 1. An example of a block Macaulay matrix $\boldsymbol{M} \in \mathbb{R}^{60\times 84}$ (degree $d = 6$) of a quadratic two-parameter eigenvalue problem ($\boldsymbol{A}_{\boldsymbol{\omega}} \in \mathbb{R}^{4\times 3}$ and $d_\mathrm{S} = 2$). The elements of the seed equation, i.e., the generating MEP, are indicated in red, while the elements of the "new" matrix equations obtained by invoking block FmSRs of total degree $d_\mathrm{R} \geq 1$ are indicated in blue (the elements not shown are zero). Vertical lines indicate the different degree blocks, while horizontal dashed lines separate block FmSRs with monomials of different total degree d_R. (For the interpretation of the colors in this figure, we refer the reader to the web version of this paper.)

$$\boldsymbol{M}(d) = \left[\!\!\left[\left\{ \prod_{i=1}^{n} \lambda_i^{d_i} \right\} \boldsymbol{\mathcal{M}}\left(\lambda_1, \ldots, \lambda_n\right) \boldsymbol{z} \right]\!\!\right],$$

where $[\![\cdot]\!]$ denotes the arrangement of the shifted coefficient matrices $\boldsymbol{A}_{\boldsymbol{\omega}}$ of the matrix equations (not the associated eigenvalues or eigenvectors). These shifted coefficient matrices are indexed both in row (different block FmSRs) and column (different associated monomials) direction by the different monomials in the eigenvalues of total degree at most d. The number of rows $p(d)$ and columns $q(d)$ of $\boldsymbol{M}(d)$ are given by

$$p(d) = k\binom{d - d_\mathrm{S} + n}{n} = k\frac{(d - d_\mathrm{S} + n)!}{n!(d - d_\mathrm{S})!} \quad \text{and} \quad q(d) = l\binom{d+n}{n} = l\frac{(d+n)!}{n!d!}.$$

The actual structure of the block Macaulay matrix depends on its multivariate monomial ordering.

Consequently, we can rewrite the MEP and the "new" matrix equations obtained via block FmSRs as a matrix-vector product of the generated block Macaulay matrix $\boldsymbol{M}(d) \in \mathbb{R}^{p(d)\times q(d)}$ and a structured vector $\boldsymbol{v}(d) \in \mathbb{C}^{q(d)\times 1}$:

$$\boldsymbol{M}(d) \begin{bmatrix} \boldsymbol{z} \\ \hline \boldsymbol{z}\lambda_1 \\ \vdots \\ \boldsymbol{z}\lambda_n \\ \hline \boldsymbol{z}\lambda_1^2 \\ \vdots \end{bmatrix} = \boldsymbol{0}.$$

We increase the degree d of the block Macaulay matrix $\boldsymbol{M}(d)$ until it is *large enough* and reaches the desired degree $d > d^*$, a concept on which we elaborate in Section 4.2. The

vector $\boldsymbol{v}(d)$ is a vector in the (right) null space of $\boldsymbol{M}(d)$ and has a block multivariate Vandermonde structure, which is *enforced* by the consecutive block FmSRs that generate the block rows of $\boldsymbol{M}(d)$. In the structure of both the null space (Section 4) and the column space (Section 5) of $\boldsymbol{M}(d)$ lies the key to solving its generating MEP. To alleviate the notational complexity in this paper, we no longer specify the degree d explicitly, but we assume it to be *large enough* (i.e., $d > d^*$).

Remark 1. Note that we make a distinction between *block rows/columns* and *degree blocks*. A block row (column) gathers all the rows (columns) that correspond to one monomial (e.g., all the rows that belong to λ_1^2), while a degree block contains all the block rows/columns that correspond to monomials of the same total degree (e.g., all the rows that belong to λ_1^2, $\lambda_1\lambda_2$, and λ_2^2). A degree block thus contains multiple block rows/columns (except when the total degree is zero or the number of variables is equal to one). We separate different degree blocks in matrices and vectors with horizontal and vertical lines, as shown in Fig. 1.

4. Null space based approach

We now exploit the structure of the null space of the block Macaulay matrix in order to find the solutions of its seed equation, i.e., the MEP that we want to solve. We show that a multidimensional realization problem in the structured null space yields the affine solutions of the MEP (Section 4.1). Afterwards, we explain the concept of a *large enough* degree and show how to deal with the solutions at infinity (Section 4.2). Finally, we summarize the different steps of the null space based algorithm (Section 4.3).

4.1. Multidimensional realization theory

We start our explanation with the block multivariate Vandermonde basis matrix (we assume that we know all the solutions), but we generalize it afterwards to any (numerical) basis matrix of the null space of the block Macaulay matrix.

4.1.1. Block multivariate Vandermonde basis matrix (theoretical multidimensional realization problem)

We consider, for didactic purposes, an MEP $\boldsymbol{\mathcal{M}}(\lambda_1, \ldots, \lambda_n)\,\boldsymbol{z} = \boldsymbol{0}$ that only has m_a simple (i.e., algebraic multiplicity is one), affine (i.e., non-infinite), and isolated solutions (i.e., the solution set is zero-dimensional). If we build a block Macaulay matrix $\boldsymbol{M}$ of *large enough* degree $d > d^*$ (see Section 4.2), then there exists a block multivariate Vandermonde vector $\boldsymbol{v}|_{(j)}$ $(j = 1, \ldots, m_a)$ in the null space of $\boldsymbol{M}$ for every solution of the MEP and, together, these basis vectors span the entire null space of $\boldsymbol{M}$. They naturally form the block multivariate Vandermonde basis matrix $\boldsymbol{V} \in \mathbb{C}^{q \times m_a}$ of degree $d > d^*$ (same degree as $\boldsymbol{M}$):

$$\boldsymbol{V} = \begin{bmatrix} \boldsymbol{v}|_{(1)} & \cdots & \boldsymbol{v}|_{(m_a)} \end{bmatrix} = \left[\begin{array}{ccc} \boldsymbol{z}|_{(1)} & \cdots & \boldsymbol{z}|_{(m_a)} \\ \hline (\lambda_1 \boldsymbol{z})|_{(1)} & \cdots & (\lambda_1 \boldsymbol{z})|_{(m_a)} \\ \vdots & & \vdots \\ (\lambda_n \boldsymbol{z})|_{(1)} & \cdots & (\lambda_n \boldsymbol{z})|_{(m_a)} \\ \hline \left(\lambda_1^2 \boldsymbol{z}\right)|_{(1)} & \cdots & \left(\lambda_1^2 \boldsymbol{z}\right)|_{(m_a)} \\ \vdots & & \vdots \end{array}\right]. \tag{5}$$

The structured $\boldsymbol{V}$ does presume that the (affine) null space of the block Macaulay matrix has a "special shift structure". Mathematically, we can write this "special shift structure" as (when we shift some (block) rows with the first eigenvalue λ_1)

$$\underbrace{\boldsymbol{S}_1 \boldsymbol{V}}_{\text{before shift}} \boldsymbol{D}_{\lambda_1} = \underbrace{\boldsymbol{S}_{\lambda_1} \boldsymbol{V}}_{\text{after shift}},$$

where the diagonal matrix $\boldsymbol{D}_{\lambda_1} \in \mathbb{C}^{m_a \times m_a}$ contains the different solutions for the eigenvalue λ_1 and the row selection matrices $\boldsymbol{S}_1$ and $\boldsymbol{S}_{\lambda_1}$ select the (block) rows before and after the shift, respectively. We say that the rows in $\boldsymbol{S}_{\lambda_1} \boldsymbol{V}$ are *hit* by the shift with λ_1. This "special shift structure" does not restrict itself to the first eigenvalue, but applies to all eigenvalues. It even holds for any shift polynomial $g(\lambda_1, \ldots, \lambda_n)$ in the eigenvalues of the MEP.[3] For example, when we shift the first three block rows of $\boldsymbol{V}$ with $2\lambda_1 + 3\lambda_2^4$:

$$\underbrace{\begin{bmatrix} \boldsymbol{z}|_{(1)} & \cdots & \boldsymbol{z}|_{(m_a)} \\ (\lambda_1 \boldsymbol{z})|_{(1)} & \cdots & (\lambda_1 \boldsymbol{z})|_{(m_a)} \\ (\lambda_2 \boldsymbol{z})|_{(1)} & \cdots & (\lambda_2 \boldsymbol{z})|_{(m_a)} \end{bmatrix}}_{\text{before shift}} \begin{bmatrix} \left(2\lambda_1 + 3\lambda_2^4\right)|_{(1)} & \cdots & 0 \\ \vdots & \ddots & \vdots \\ 0 & \cdots & \left(2\lambda_1 + 3\lambda_2^4\right)|_{(m_a)} \end{bmatrix} =$$

$$\underbrace{2 \begin{bmatrix} (\lambda_1 \boldsymbol{z})|_{(1)} & \cdots & (\lambda_1 \boldsymbol{z})|_{(m_a)} \\ \left(\lambda_1^2 \boldsymbol{z}\right)|_{(1)} & \cdots & \left(\lambda_1^2 \boldsymbol{z}\right)|_{(m_a)} \\ (\lambda_1 \lambda_2 \boldsymbol{z})|_{(1)} & \cdots & (\lambda_1 \lambda_2 \boldsymbol{z})|_{(m_a)} \end{bmatrix} + 3 \begin{bmatrix} \left(\lambda_2^4 \boldsymbol{z}\right)|_{(1)} & \cdots & \left(\lambda_2^4 \boldsymbol{z}\right)|_{(m_a)} \\ \left(\lambda_1 \lambda_2^4 \boldsymbol{z}\right)|_{(1)} & \cdots & \left(\lambda_1 \lambda_2^4 \boldsymbol{z}\right)|_{(m_a)} \\ \left(\lambda_2^5 \boldsymbol{z}\right)|_{(1)} & \cdots & \left(\lambda_2^5 \boldsymbol{z}\right)|_{(m_a)} \end{bmatrix}}_{\text{after shift}}.$$

Hence, we obtain the expression

$$(\boldsymbol{S}_g \boldsymbol{V}) = (\boldsymbol{S}_1 \boldsymbol{V}) \boldsymbol{D}_g, \tag{6}$$

[3] Shifting with a polynomial instead of a simple eigenvalue can be interesting in some practical situations: consider the case where the solutions of the MEP characterize the stationary points of a polynomial objective function in the eigenvalues, then the smallest evaluation of this polynomial objective function (i.e., the smallest diagonal element of $\boldsymbol{D}_g$) corresponds to the minimum of the underlying optimization problem. Conversely, we want to limit the total degree of the shift polynomial from a computational point of view (and use only linear shift polynomials), as a higher total degree of the shift polynomial requires a larger degree of the block Macaulay matrix (see Section 4.2 to understand why the degree d has to be *large enough*).

where the diagonal matrix $\boldsymbol{D}_g \in \mathbb{C}^{m_a \times m_a}$ contains the evaluations of the shift polynomial $g(\lambda_1, \ldots, \lambda_n)$ in the different solutions of the MEP. In order for this expression to cover all the affine solutions, the row selection matrix $\boldsymbol{S}_1 \in \mathbb{R}^{m_a \times q}$ has to select m_a linearly independent rows from $\boldsymbol{V}$ (then $\boldsymbol{S}_1\boldsymbol{V}$ is square and non-singular). Actually, from algebraic geometry and from earlier work on the traditional Macaulay matrix, it follows that these linearly independent rows correspond to the (affine) standard monomials [4,17,23]. The *row combination matrix*[4] $\boldsymbol{S}_g \in \mathbb{R}^{m_a \times q}$, on the other hand, simply selects the linear combinations of rows hit by the shift with $g(\lambda_1, \ldots, \lambda_n)$.

4.1.2. Numerical basis matrix (practical multidimensional realization problem)

In practice, we do not know the block multivariate Vandermonde basis matrix $\boldsymbol{V}$ in advance, since it is constructed from the unknown solutions of the MEP. We work instead with a numerical basis matrix $\boldsymbol{Z} \in \mathbb{C}^{q \times m_a}$ of the null space of the block Macaulay matrix $\boldsymbol{M}$, for example obtained via the singular value decomposition. Before translating the theoretical multidimensional realization problem into a practical one, we make this "special shift structure" more concrete.

Proposition 1 *(**Backward block multi-shift-invariance** – Appendix A). The (affine) null space of the block Macaulay matrix is **backward block multi-shift-invariant**. This means that if we select a block row of a basis matrix of the null space and multiply/shift this block row with one of the eigenvalues, then we obtain another block row of that basis matrix (when the degree is large enough).*

Backward block multi-shift-invariance is a property of the null space as a vector space and not of a specific basis matrix (see Appendix A), hence we can also use a numerical basis matrix $\boldsymbol{Z}$. There exists a linear transformation $\boldsymbol{T}$ between both basis matrices, namely $\boldsymbol{V} = \boldsymbol{Z}\boldsymbol{T}$, with $\boldsymbol{T} \in \mathbb{C}^{m_a \times m_a}$ a non-singular transformation matrix, which transforms (6) into a solvable GEP,

$$(\boldsymbol{S}_g\boldsymbol{Z})\,\boldsymbol{T} = (\boldsymbol{S}_1\boldsymbol{Z})\,\boldsymbol{T}\boldsymbol{D}_g, \tag{7}$$

where $\boldsymbol{T}$ contains the eigenvectors and $\boldsymbol{D}_g$ the eigenvalues of the matrix pencil $(\boldsymbol{S}_g\boldsymbol{Z}, \boldsymbol{S}_1\boldsymbol{Z})$. Alternatively, we can also consider the SEP

$$(\boldsymbol{S}_1\boldsymbol{Z})^{-1}\,(\boldsymbol{S}_g\boldsymbol{Z})\,\boldsymbol{T} = \boldsymbol{T}\boldsymbol{D}_g. \tag{8}$$

We can then use the matrix of eigenvectors $\boldsymbol{T}$ to obtain $\boldsymbol{V}$ (via $\boldsymbol{V} = \boldsymbol{Z}\boldsymbol{T}$), and hence, find the affine solutions of the MEP. The null space of the block Macaulay matrix can be interpreted as the column space of a multidimensional observability matrix [25,50].

[4] When the shift is merely a monomial of (some of the) eigenvalues, the row combination matrix $\boldsymbol{S}_g$ is a row selection matrix because every shift only hits one row.

In that setting, it is possible to view this null space based solution approach as an exact multidimensional realization problem in that null space (see Appendix A).

Influence of affine solutions with a multiplicity larger than one When all solutions are simple, we find one column in the block multivariate Vandermonde basis matrix $\boldsymbol{V}$ of the null space for every solution of the MEP and every solution/column contributes to the nullity of the block Macaulay matrix. However, if multiple (affine and isolated) solutions prevail, the null space of the block Macaulay matrix no longer contains only the block multivariate Vandermonde solution vectors, but also linear combinations of the partial derivatives of these solution vectors, i.e., we have a confluent block multivariate Vandermonde basis matrix (Dayton et al. [18] and Möller and Stetter [39] give an elaborate exposition in the case of systems of multivariate polynomial equations). The SEP in (8) is defective and a proper analysis requires the Jordan normal form and the confluent block multivariate Vandermonde matrix [6]. In practice, since we work with floating-point algorithms to compute the SEP in (8), we still find numerical approximations of the multiple eigentuples and eigenvectors, but we experience a loss of numerical accuracy in computing them [27]. Alternatively, we can consider n different shift polynomials $g_i(\lambda_1, \ldots, \lambda_n)$, e.g., shifting with every eigenvalue λ_i, and use n Schur decompositions to accurately obtain the different components of the eigentuples [6,16].

4.2. Concept of a large enough degree

One central question remains unanswered in the above-described approach: "When is the degree d *large enough*?" When we increase the degree d by invoking more block FmSRs, we notice that the nullity of the block Macaulay matrix $\boldsymbol{M}$ (i.e., the dimension of its null space) stabilizes at the total number of solutions m_b in the case of a zero-dimensional solution set. It is possible to monitor this behavior by checking the nullity of $\boldsymbol{M}$ for increasing d. When the degree $d = d^*$, any basis matrix of the null space has m_b linearly independent columns and, when checking the rank of this basis matrix from top to bottom, at least one linearly independent row per degree block. The structure of a basis matrix for $d > d^*$ depends on whether the MEP has only affine solutions or affine solutions and solutions at infinity (see Fig. 2).

Only affine solutions When the MEP only has affine solutions ($m_b = m_a$), these linearly independent rows correspond to the affine standard monomials. For larger degrees $d > d^*$, they remain stable at their respective positions and new degree blocks contain no additional linearly independent rows (see Fig. 2a). We identify two zones in the basis matrix: a *regular zone* that contains the linearly independent rows related to the affine standard monomials and a *gap zone* without additional linearly independent rows.

Affine solutions and solutions at infinity An MEP can also have solutions at infinity, due to the singularity of some higher degree coefficient matrices. The nullity of the block

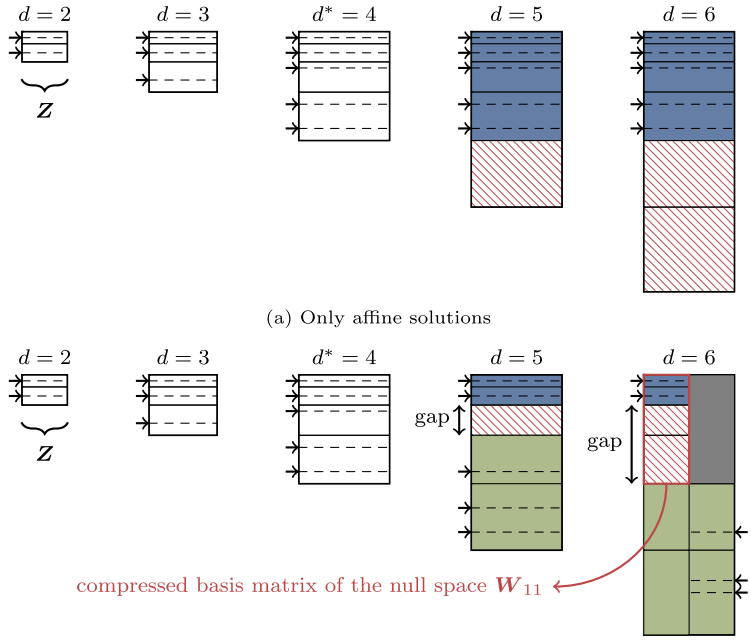

Fig. 2. A basis matrix of the null space of a block Macaulay matrix $\boldsymbol{M}$, which grows by invoking more block FmSRs (increasing d). At a certain degree d^* (in this example $d^* = 4$), the nullity stabilizes at the total number of solutions m_b. In the situation with only affine solutions (Fig. 2a), the linearly independent rows of the basis matrix, checked from top to bottom, correspond to the affine standard monomials and stabilize at their respective positions (indicated by dashed lines). New degree blocks contain no additional linearly independent rows when $d > d^*$. When the MEP has solutions at infinity (Fig. 2b), the linearly independent rows of the basis matrix that correspond to the standard monomials related to the solutions at infinity (also indicated by dashed lines) move to higher degree blocks when $d > d^*$. A gap in the rows emerges that separates these two types of linearly independent rows, and the influence of the solutions at infinity can be deflated via a column compression.

Macaulay matrix after stabilization corresponds to the total number of solutions m_b of the MEP, which is now the sum of the affine solutions and the solutions at infinity ($m_b = m_a + m_\infty$). Every solution spans one basis vector in this null space, hence all the columns of the numerical basis matrix are linear combinations of affine solutions and solutions at infinity. Next to the affine standard monomials, also linearly independent rows related to the standard monomials that correspond to solutions at infinity appear in the basis matrix. When we increase the degree ($d > d^*$), the linearly independent rows that correspond to the affine standard monomials remain again stable at their respective positions, but the standard monomials that correspond to the solutions at infinity move to higher degree blocks when the block FmSRs proceed (see Fig. 2b). Eventually, a gap in the rows emerges that separates both types of linearly independent rows. This gap grows when we keep increasing the degree $d > d^*$. Now, we observe three zones in the basis matrix: a regular zone, a gap zone, and a *singular zone* that contains the linearly independent rows related to the standard monomials that correspond to the solutions at infinity. Via a column compression [23], we can deflate the solutions at infinity and use

the affine null space based approach as if no solutions at infinity are present (we simply replace $\boldsymbol{Z}$ in (7) by $\boldsymbol{W}_{11}$).

Definition 4 *(**Column compression**).* A numerical basis matrix $\boldsymbol{Z} = \begin{bmatrix} \boldsymbol{Z}_1^{\mathrm{T}} & \boldsymbol{Z}_2^{\mathrm{T}} \end{bmatrix}^{\mathrm{T}}$ of the null space of the block Macaulay matrix $\boldsymbol{M}$ is a $q \times m_b$ matrix, which can be partitioned into a $s \times m_b$ matrix $\boldsymbol{Z}_1$ (that contains the regular zone and gap zone) and a $(q-s) \times m_b$ matrix $\boldsymbol{Z}_2$ (that contains the singular zone), with $\operatorname{rank}(\boldsymbol{Z}_1) = m_a < m_b$. Furthermore, let the singular value decomposition of $\boldsymbol{Z}_1 = \boldsymbol{U}\boldsymbol{\Sigma}\boldsymbol{Q}^{\mathrm{T}}$. Then, $\boldsymbol{W} = \boldsymbol{Z}\boldsymbol{Q}$ is called the **column compression** of $\boldsymbol{Z}$ and can be partitioned as

$$\boldsymbol{W} = \begin{bmatrix} \boldsymbol{W}_{11} & \boldsymbol{0} \\ \boldsymbol{W}_{21} & \boldsymbol{W}_{22} \end{bmatrix},$$

where $\boldsymbol{W}_{11}$ is the $s \times m_a$ compressed numerical basis matrix of the null space.

When we want to shift the linearly independent rows that correspond to the affine standard monomials in (6) with a shift polynomial $g(\lambda_1, \ldots, \lambda_n)$ of degree d_g, the gap zone needs to be able to *accommodate* this shift, which means that the rows that correspond to the monomials with the highest total degree hit by the shift must be present in the gap zone. Hence, the degree d of the block Macaulay matrix is *large enough* when $d \geq d^* + d_g$.

4.3. Null space based algorithm

Algorithm 1 Null space based approach.

1: Recursively enlarge the block Macaulay matrix $\boldsymbol{M}$ until its nullity has stabilized and the gap can accommodate the (user-defined) shift polynomial, i.e., the degree d is *large enough* (Section 4.2).
2: Compute a numerical basis matrix $\boldsymbol{Z}$ of the null space of $\boldsymbol{M}$.
3: Determine the gap and the number of affine solutions m_a via row-wise rank checks from top to bottom in $\boldsymbol{Z}$ (Section 4.2).
4: Use Definition 4 to obtain the compressed numerical basis matrix $\boldsymbol{W}_{11}$ of the null space.
5: For a (user-defined) shift polynomial $g(\lambda_1, \ldots, \lambda_n)$ and $\boldsymbol{W}_{11}$ that can accommodate the shift (i.e., $d \geq d^* + d_g$), solve the GEP

$$(\boldsymbol{S}_g \boldsymbol{W}_{11})\, \boldsymbol{T} = (\boldsymbol{S}_1 \boldsymbol{W}_{11})\, \boldsymbol{T} \boldsymbol{D}_g,$$

where the matrices $\boldsymbol{S}_1$, $\boldsymbol{S}_g$, $\boldsymbol{T}$, and $\boldsymbol{D}_g$ are defined as in (7).
6: Retrieve the solutions from the (affine) block multivariate Vandermonde basis matrix $\boldsymbol{V} = \boldsymbol{W}_{11}\boldsymbol{T}$.

Remark 2. Since we only select linearly independent rows and not block rows from the numerical basis matrix $\boldsymbol{Z}$, we do not fully exploit the backward block multi-shift-invariance of the null space. Furthermore, row-wise rank checks from top to bottom to identify the linearly independent rows are numerically not very robust. However, instead of selecting m_a linearly independent rows of $\boldsymbol{Z}$, the row selection matrix $\boldsymbol{S}_1 \in \mathbb{R}^{m \times q}$ can also select entire block rows of $\boldsymbol{Z}$ (but needs to contain at least m_a linearly independent rows

to cover all the affine solutions). Because of the block multi-shift-invariance, the row combination matrix $\boldsymbol{S}_g \in \mathbb{R}^{m \times q}$ also selects entire block rows of $\boldsymbol{Z}$. Mathematically, we consider a rectangular matrix pencil $(\boldsymbol{S}_g\boldsymbol{Z}, \boldsymbol{S}_1\boldsymbol{Z})$ or use the pseudo-inverse $(.^\dagger)$ to obtain a solvable SEP

$$(\boldsymbol{S}_1\boldsymbol{Z})^\dagger (\boldsymbol{S}_g\boldsymbol{Z})\, \boldsymbol{T} = \boldsymbol{T}\boldsymbol{D}_g.$$

Shifting entire block rows (or degree blocks) replaces the row-wise rank checks by more efficient (degree) block row-wise rank checks.

5. Column space based approach

In this section, we consider the column space of the block Macaulay matrix instead of its null space. The intrinsic complementarity between both fundamental subspaces (Section 5.1) enables a new, complementary algorithm to solve MEPs, which works directly on the sparse and structured data (Section 5.2). We summarize the different steps of the column space based algorithm, but we do not elaborate in detail on exploiting the sparsity and structure (Section 5.3).

5.1. Complementarity between the null space and the column space of a matrix

The null space and column space of an arbitrary matrix share an intrinsic complementarity. We give the following lemma without proof [23, p. 41]:

Lemma 1 *(**Complementarity of linearly independent rows and columns**). Consider a matrix $\boldsymbol{M} \in \mathbb{R}^{p \times q}$, with $\operatorname{rank}(\boldsymbol{M}) = r < \min(p, q)$. Let $\boldsymbol{Z} \in \mathbb{C}^{q \times (q-r)}$ be a full column rank matrix, the columns of which generate a basis matrix of the null space of $\boldsymbol{M}$: $\boldsymbol{M}\boldsymbol{Z} = \boldsymbol{0}$. Using a row permutation matrix $\boldsymbol{P}$, reorder the rows of $\boldsymbol{Z}$ into $\boldsymbol{P}\boldsymbol{Z} = \begin{bmatrix}\boldsymbol{Z}_A^{\mathrm{T}} & \boldsymbol{Z}_B^{\mathrm{T}}\end{bmatrix}^{\mathrm{T}}$, where the submatrix $\boldsymbol{Z}_A$ contains exactly $q - r$ linearly independent rows, and partition the columns of the matrix $\boldsymbol{M}$ accordingly with $\boldsymbol{P}^{-1}$ so that $\boldsymbol{M}\boldsymbol{P}^{-1} = [\boldsymbol{M}_A \quad \boldsymbol{M}_B]$: $\boldsymbol{M}\boldsymbol{Z} = \boldsymbol{M}\boldsymbol{P}^{-1}\boldsymbol{P}\boldsymbol{Z} = \boldsymbol{M}_A\boldsymbol{Z}_A + \boldsymbol{M}_B\boldsymbol{Z}_B = \boldsymbol{0}$. Then*

$$\operatorname{rank}(\boldsymbol{M}_B) = r \Leftrightarrow \operatorname{rank}(\boldsymbol{Z}_A) = q - r.$$

The choice of the row permutation matrix $\boldsymbol{P}$ is not unique, there exist many possibilities to identify $q - r$ linearly independent rows in $\boldsymbol{Z}$. This lemma expresses a complementarity for maximal sets of linearly independent rows in $\boldsymbol{Z}$ with respect to maximal sets of linearly independent columns in $\boldsymbol{M}$. Obviously, we have $\boldsymbol{M}_A\boldsymbol{Z}_A = -\boldsymbol{M}_B\boldsymbol{Z}_B$, such that $\boldsymbol{M}_A = \boldsymbol{M}_B\left(\boldsymbol{Z}_B\boldsymbol{Z}_A^{-1}\right)$ expresses the linearly dependent columns of $\boldsymbol{M}$ as a linear combination of the linearly independent ones and $\boldsymbol{Z}_B = -\left(\boldsymbol{M}_B^\dagger\boldsymbol{M}_A\right)\boldsymbol{Z}_A$ expresses the linearly dependent rows of $\boldsymbol{Z}$ as a linear combination of the selected linearly independent ones. This lemma leads to an important observation: when we index the

linearly independent rows of $\boldsymbol{Z}$ (row-wise from top to bottom), it turns out that the "corresponding" columns of $\boldsymbol{M}$ are linearly dependent columns on the other columns of $\boldsymbol{M}$ (column-wise from right to left), as the next example illustrates.

Example 8. We consider a matrix $\boldsymbol{M} \in \mathbb{R}^{4\times 7}$ and a basis matrix of its null space $\boldsymbol{Z} \in \mathbb{C}^{7\times 3}$:

$$\boldsymbol{M}\boldsymbol{Z} = \begin{bmatrix} 2 & 0 & 0 & 1 & 0 & 3 & -3 \\ 4 & -6 & 0 & 2 & 0 & 0 & 0 \\ -4 & 0 & 2 & 0 & -6 & 0 & 0 \\ 2 & 0 & 0 & 0 & 2 & 6 & -6 \end{bmatrix} \begin{bmatrix} 0 & 0 & -1 \\ 0 & 1 & 1 \\ 0 & 9 & -1 \\ 0 & 3 & -2 \\ 0 & 3 & -1 \\ -1 & 0 & 0 \\ -1 & 0 & 0 \end{bmatrix} = \boldsymbol{0}.$$

The linearly independent rows of $\boldsymbol{Z}$, checked from top to bottom, are indexed as $\{1, 2, 6\}$. On the other hand, the linearly dependent columns of $\boldsymbol{M}$, checked from right to left, are also indexed as $\{1, 2, 6\}$, in accordance to Lemma 1.

We can now apply Lemma 1 to the block Macaulay matrix and any basis matrix of its null space. Observe that we can replace $\boldsymbol{Z}$ by a linear transformation $\boldsymbol{Z}\boldsymbol{T}$, so Lemma 1 is independent of the choice of basis matrix of the null space. The solutions of the MEP give rise to standard monomials, which are visible in both the null space and the column space of the block Macaulay matrix. When we check the rank of the basis matrix row-wise from top to bottom, every linearly independent row corresponds to exactly one standard monomial. Similarly, every linearly dependent column of the block Macaulay matrix, checked from right to left, also corresponds to exactly one standard monomial. Fig. 3 visualizes the complementarity between both fundamental subspaces. Note that the gap in the basis matrix of the null space is a gap of linearly dependent rows, while the gap in the block Macaulay matrix is a gap of linearly independent columns.

5.2. Equivalent column space realization theory

We consider again a block Macaulay matrix $\boldsymbol{M} \in \mathbb{R}^{p\times q}$, with *large enough* degree $d \geq d^* + d_g$, and a numerical basis matrix $\boldsymbol{W} \in \mathbb{C}^{q\times m_b}$ of its null space after a column compression (see Definition 4). When we shift the linearly independent rows of the compressed basis matrix $\boldsymbol{W}_{11}$ with a shift polynomial $g(\lambda_1, \ldots, \lambda_n)$, we obtain again

$$(\boldsymbol{S}_g \boldsymbol{W}_{11})\,\boldsymbol{T} = (\boldsymbol{S}_1 \boldsymbol{W}_{11})\,\boldsymbol{T}\boldsymbol{D}_g, \tag{9}$$

where the matrices $\boldsymbol{S}_1$, $\boldsymbol{S}_g$, $\boldsymbol{T}$, and $\boldsymbol{D}_g$ are defined as in (7). Next, we define two new matrices $\boldsymbol{B}$ and $\boldsymbol{C}$. The matrix $\boldsymbol{B} \in \mathbb{C}^{m_a\times m_a}$ contains all the linearly independent rows of the matrix $\boldsymbol{W}_{11}$, which corresponds to the selection $\boldsymbol{S}_1\boldsymbol{W}_{11}$, and is partitioned so that each of its top $m_h = m_a - m_c$ rows (denoted by $\boldsymbol{B}_1$) only hits rows inside $\boldsymbol{B}$ after

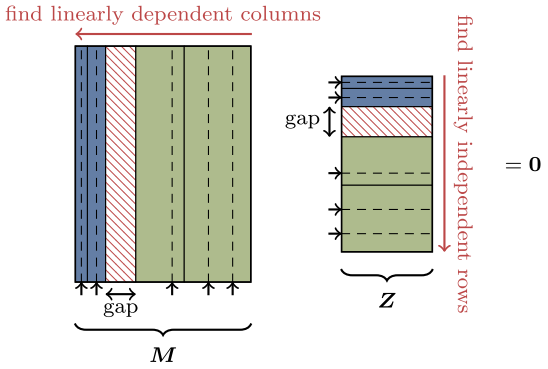

Fig. 3. If we check the rank of a basis matrix $\boldsymbol{Z}$ of the null space of the block Macaulay matrix $\boldsymbol{M}$ row-wise from top to bottom, every linearly independent row corresponds to one standard monomial (indicated by dashed lines). Because of the complementarity between the null space and column space, the linearly dependent columns of $\boldsymbol{M}$ (also indicated by dashed lines), checked column-wise from right to left, correspond to the same standard monomials.

shifting with $g(\lambda_1, \ldots, \lambda_n)$ and each of its bottom m_c rows (denoted by $\boldsymbol{B}_2$) hits at least one row not in $\boldsymbol{B}$. We gather the m_c linear combinations of rows hit by shifting the rows of $\boldsymbol{B}_2$ in the matrix $\boldsymbol{C} \in \mathbb{C}^{m_c \times m_a}$ and rewrite (9) as a matrix pencil $(\boldsymbol{A}, \boldsymbol{B})$,

$$\underbrace{\begin{bmatrix} \boldsymbol{S}_g' \boldsymbol{B} \\ \boldsymbol{C} \end{bmatrix}}_{\boldsymbol{A}} \boldsymbol{T} = \underbrace{\begin{bmatrix} \boldsymbol{B}_1 \\ \boldsymbol{B}_2 \end{bmatrix}}_{\boldsymbol{B}} \boldsymbol{T} \boldsymbol{D}_g,$$

where shifting the rows in $\boldsymbol{B}_1$ leads to linear combinations of rows only in $\boldsymbol{B}$ ($\boldsymbol{B}_1 \to \boldsymbol{S}_g' \boldsymbol{B}$) and shifting the rows in $\boldsymbol{B}_2$ leads to linear combinations of rows in $\boldsymbol{B}$ and/or not in $\boldsymbol{B}$ ($\boldsymbol{B}_2 \to \boldsymbol{C}$), with $\boldsymbol{S}_g'$ the $m_h \times m_a$ row combination matrix that selects the $m_h = m_a - m_c$ linear combinations of rows in $\boldsymbol{B}$ hit by shifting the rows of $\boldsymbol{B}_1$. For example, if we shift the τth row of $\boldsymbol{B}_2$ and $g(\lambda_1, \ldots, \lambda_n)$ hits the μth row of $\boldsymbol{B}$ ($\boldsymbol{b}_\mu$) and the νth row of $\boldsymbol{W}$ ($\boldsymbol{w}_\nu$ – not in $\boldsymbol{B}$), then the τth row of $\boldsymbol{C}$ is equal to $c_\mu \boldsymbol{b}_\mu + c_\nu \boldsymbol{w}_\nu$ (the coefficients c_μ and c_ν come from the shift polynomial). The matrix $\boldsymbol{D}_g$ is again a diagonal matrix that contains the evaluations of the shift polynomial $g(\lambda_1, \ldots, \lambda_n)$ in the different eigenvalue solutions. We can extract the matrix $\boldsymbol{B}$ from the column matrix in the left-hand side, after which an SEP appears (with $\boldsymbol{BT}$ as its matrix of eigenvectors):

$$\begin{bmatrix} \boldsymbol{S}_g' \\ \boldsymbol{C}\boldsymbol{B}^{-1} \end{bmatrix} \boldsymbol{BT} = \boldsymbol{BT} \boldsymbol{D}_g. \tag{10}$$

The matrix $\boldsymbol{B}$ is invertible because it contains m_a linearly independent rows by construction (the rows that correspond to the affine standard monomials). In the remainder of this section, we translate (10) to the column space via Lemma 1, avoiding the computation of a numerical basis matrix of the null space.

The matrices $\boldsymbol{B}$ and $\boldsymbol{C}$ contain rows (or linear combinations of rows) of the matrix $\boldsymbol{W}_{11}$. We define the matrix $\boldsymbol{D} \in \mathbb{C}^{m_r \times m_a}$ (with $m_r = s - m_a - m_c$) as the matrix that

contains the remaining rows of $\boldsymbol{W}_{11}$, such that every row of $\boldsymbol{W}_{11}$ is *represented* once in $\boldsymbol{B}$, $\boldsymbol{C}$, or $\boldsymbol{D}$. For example, if a row in $\boldsymbol{C}$ contains a linear combination of multiple rows of $\boldsymbol{W}$, then that row of $\boldsymbol{C}$ represents only one of those rows in the linear combination. The other rows of the linear combination need to be represented by other rows of $\boldsymbol{C}$, or they are included in $\boldsymbol{B}$ or $\boldsymbol{D}$. Consequently, we can rearrange the basis matrix $\boldsymbol{W}$ as

$$\boldsymbol{P}\boldsymbol{W} = \begin{bmatrix} \boldsymbol{B} & \boldsymbol{0} \\ \boldsymbol{C} & \boldsymbol{0} \\ \boldsymbol{D} & \boldsymbol{0} \\ \boldsymbol{W}_{21} & \boldsymbol{W}_{22} \end{bmatrix},$$

where the matrix $\boldsymbol{P}$ is a $q \times q$ row combination matrix that is invertible (because it is square and of full column rank by construction) and does not alter the rank structure of $\boldsymbol{W}$ (because it takes linear combinations of rows that already depend linearly on the rows in $\boldsymbol{B}$). Using Lemma 1, we can rearrange the columns of the block Macaulay matrix in accordance to the rearranged basis matrix of the null space and obtain

$$\underbrace{\begin{bmatrix} \boldsymbol{N}_1 & \boldsymbol{N}_2 & \boldsymbol{N}_3 & \boldsymbol{N}_4 \end{bmatrix}}_{\boldsymbol{N}} \begin{bmatrix} \boldsymbol{B} & \boldsymbol{0} \\ \boldsymbol{C} & \boldsymbol{0} \\ \boldsymbol{D} & \boldsymbol{0} \\ \boldsymbol{W}_{21} & \boldsymbol{W}_{22} \end{bmatrix} = \boldsymbol{0}, \tag{11}$$

where every matrix $\boldsymbol{N}_i \in \mathbb{R}^{p \times q_i}$ corresponds to a subset of the columns (or linear combinations of columns) of $\boldsymbol{M}$. We call $\boldsymbol{N} = \boldsymbol{M}\boldsymbol{P}^{-1} \in \mathbb{R}^{p \times q}$ the *rearranged* block Macaulay matrix. Now, we apply a backward QR-decomposition[5] on $\boldsymbol{N}$, which yields

$$\boldsymbol{Q} \begin{bmatrix} \boldsymbol{R}_{14} & \boldsymbol{R}_{13} & \boldsymbol{R}_{12} & \boldsymbol{R}_{11} \\ \boldsymbol{R}_{24} & \boldsymbol{R}_{23} & \boldsymbol{R}_{22} & \boldsymbol{0} \\ \boldsymbol{R}_{34} & \boldsymbol{R}_{33} & \boldsymbol{0} & \boldsymbol{0} \\ \boldsymbol{R}_{44} & \boldsymbol{0} & \boldsymbol{0} & \boldsymbol{0} \end{bmatrix} \begin{bmatrix} \boldsymbol{B} & \boldsymbol{0} \\ \boldsymbol{C} & \boldsymbol{0} \\ \boldsymbol{D} & \boldsymbol{0} \\ \boldsymbol{W}_{21} & \boldsymbol{W}_{22} \end{bmatrix} = \boldsymbol{0},$$

or, if we pre-multiply both sides by $\boldsymbol{Q}^{-1} = \boldsymbol{Q}^{\mathrm{T}}$ (the labels denote the number of rows/columns of the different blocks[6]),

[5] Essentially, the backward QR-decomposition triangularizes the rearranged matrix $\boldsymbol{N}$ as the traditional forward QR-decomposition, but starts with the last column of $\boldsymbol{N}$ and iteratively works towards the first column of $\boldsymbol{N}$. Its result is similar to the result of the traditional forward QR-decomposition of the matrix with all its columns flipped.

[6] A closer analysis of the upper triangular matrix $\boldsymbol{R}$ reveals two special cases. Firstly, $\boldsymbol{W}_{21}$ and $\boldsymbol{W}_{22}$ are absent from $\boldsymbol{W}$ when there are no solutions at infinity. As a consequence, (11) no longer contains $\boldsymbol{N}_4$ and $q - s = 0$, which means that we can ignore the first block row and last block column of $\boldsymbol{R}$ (see the numerical example in Section 6.1). Secondly, the size of the block Macaulay matrix $\boldsymbol{M}$ determines the size of $\boldsymbol{R}_{44}$: when $p > q$ the matrix $\boldsymbol{R}_{44}$ is tall, when $p < q$ the matrix $\boldsymbol{R}_{44}$ is wide, and when $p = q - m_a$ the matrix $\boldsymbol{R}_{44}$ is absent (see the numerical example in Section 6.2). Note that it can even happen that $p = q - m_b < q - m_a$ when the MEP has solutions at infinity: then we need to use a larger degree d or remove the linearly dependent columns in $\boldsymbol{N}_4$, which correspond to the standard monomials related to the solutions at infinity, to ensure that $p \geq q - m_a$ and to obtain the structure of $\boldsymbol{R}$ as presented in (12) (see the numerical example in Section 6.4).

$$\begin{array}{r} \\ q-s \\ m_r \\ m_c \\ p-q+m_a \end{array} \begin{array}{c} \begin{array}{cccc} m_a & m_c & m_r & q-s \end{array} \\ \begin{bmatrix} \boldsymbol{R}_{14} & \boldsymbol{R}_{13} & \boldsymbol{R}_{12} & \boldsymbol{R}_{11} \\ \boldsymbol{R}_{24} & \boldsymbol{R}_{23} & \boldsymbol{R}_{22} & \boldsymbol{0} \\ \boldsymbol{R}_{34} & \boldsymbol{R}_{33} & \boldsymbol{0} & \boldsymbol{0} \\ \boldsymbol{R}_{44} & \boldsymbol{0} & \boldsymbol{0} & \boldsymbol{0} \end{bmatrix} \end{array} \begin{bmatrix} \boldsymbol{B} & \boldsymbol{0} \\ \boldsymbol{C} & \boldsymbol{0} \\ \boldsymbol{D} & \boldsymbol{0} \\ \boldsymbol{W}_{21} & \boldsymbol{W}_{22} \end{bmatrix} = \boldsymbol{0}. \tag{12}$$

We notice that $\boldsymbol{R}_{33}\boldsymbol{C} = -\boldsymbol{R}_{34}\boldsymbol{B}$, which means that

$$\boldsymbol{C}\boldsymbol{B}^{-1} = -\boldsymbol{R}_{33}^{-1}\boldsymbol{R}_{34},$$

because $\boldsymbol{R}_{33}$ is always of full rank (since the rows of $\boldsymbol{C}$ depend linearly on the rows of $\boldsymbol{B}$ and the complementarity of Lemma 1). Note that $\boldsymbol{R}_{44}$ is always a zero matrix for the same reasons (since the rows of $\boldsymbol{B}$ are linearly independent and the complementarity of Lemma 1). This relation helps to remove the dependency on the null space in (10) and yields a solvable SEP in the column space (with $\boldsymbol{H} = \boldsymbol{B}\boldsymbol{T}$),

$$\begin{bmatrix} \boldsymbol{S}_g' \\ -\boldsymbol{R}_{33}^{-1}\boldsymbol{R}_{34} \end{bmatrix} \boldsymbol{H} = \boldsymbol{H}\boldsymbol{D}_g,$$

or a GEP (to avoid the computation of the inverse of $\boldsymbol{R}_{33}$),

$$\begin{bmatrix} \boldsymbol{S}_g' \\ -\boldsymbol{R}_{34} \end{bmatrix} \boldsymbol{H} = \begin{bmatrix} \boldsymbol{I}_{m_h} & \boldsymbol{0} \\ \boldsymbol{0} & \boldsymbol{R}_{33} \end{bmatrix} \boldsymbol{H}\boldsymbol{D}_g, \tag{13}$$

with $\boldsymbol{I}_{m_h} \in \mathbb{N}^{m_h \times m_h}$ the identity matrix. The matrix of eigenvector $\boldsymbol{H} = \boldsymbol{B}\boldsymbol{T}$ corresponds to the partitioned linearly independent rows of the (affine) Vandermonde basis matrix $\boldsymbol{V}$, because the non-singular transformation matrix $\boldsymbol{T}$ relates the rows of the numerical basis matrix $\boldsymbol{W}_{11}$ (or $\boldsymbol{B}$) to the rows of $\boldsymbol{V}$. Consequently, the eigenvalues in $\boldsymbol{D}_g$ and eigenvectors in $\boldsymbol{H}$ yield the solutions of the MEP. Note that this complementary column space based approach does not require a column compression to deflate the solutions at infinity, because the backward (Q-less) QR-decomposition already separates them implicitly.

5.3. Column space based algorithm

Remark 3. Note that, when the shift polynomial $g(\lambda_1, \ldots, \lambda_n)$ is merely a monomial of (some of the) eigenvalues, the row combination matrix $\boldsymbol{P}$ is a row permutation matrix (every hit consists of only one row), and its inverse $\boldsymbol{P}^{-1}$ is equal to its transpose $\boldsymbol{P}^{\mathrm{T}}$. Applying $\boldsymbol{P}^{\mathrm{T}}$ to the block Macaulay matrix $\boldsymbol{M}$ corresponds to reordering the columns of $\boldsymbol{M}$ in accordance to $\boldsymbol{P}\boldsymbol{W}$, which is quite easy to implement.

Remark 4. Contrary to the null space based approach where we retrieve the different components of the solutions from the (affine) block multivariate Vandermonde basis

Algorithm 2 Column space based approach.

1: Recursively enlarge the block Macaulay matrix $\boldsymbol{M}$ until its nullity has stabilized and the gap can accommodate the (user-defined) shift polynomial, i.e., the degree d is *large enough* (Section 4.2).
2: Determine the linearly dependent columns via rank checks from right to left and rearrange $\boldsymbol{M}$ as in (11).
3: Compute the (Q-less) backward QR-decomposition of the rearranged block Macaulay matrix $\boldsymbol{N}$.
4: For a (user-defined) shift polynomial $g(\lambda_1, \ldots, \lambda_n)$, solve the GEP

$$\begin{bmatrix} \boldsymbol{S}'_g \\ -\boldsymbol{R}_{34} \end{bmatrix} \boldsymbol{H} = \begin{bmatrix} \boldsymbol{I}_{m_h} & \boldsymbol{0} \\ \boldsymbol{0} & \boldsymbol{R}_{33} \end{bmatrix} \boldsymbol{H} \boldsymbol{D}_g,$$

where the matrices $\boldsymbol{S}'_g$, $\boldsymbol{I}_{m_h}$, $\boldsymbol{R}_{33}$, $\boldsymbol{R}_{34}$, and $\boldsymbol{D}_g$ are defined as in (13).
5: Retrieve the solutions from the eigenvalues in $\boldsymbol{D}_g$ and the eigenvectors in $\boldsymbol{H}$ (see Remark 4).

matrix $\boldsymbol{V}$, the matrix $\boldsymbol{H}$ in the column space based approach does not necessarily contain all the components of the solutions. Therefore, we need to choose one or multiple shift polynomials $g_i(\lambda_1, \ldots, \lambda_n)$ so that the matrices $\boldsymbol{D}_{g_i}$ yield the remaining components (see the numerical example in Section 6.2). One strategy is to always shift with the n different eigenvalues, which results in n GEPs that yield the n different components of the (affine) solutions. Note that, in order to obtain accurate solutions in the presence of multiplicities, we can also apply this strategy in the null space based approach [16,6].

6. Numerical examples

In this section, we present several numerical examples to illustrate the column space based algorithm and to compare it with its null space based counterpart.

6.1. Linear two-parameter eigenvalue problem with affine solutions only

In our first numerical example, we consider the linear 2-EP from Example 4 and use a shift polynomial $g(\lambda_1, \lambda_2) = 4\lambda_2^3$ for didactic purposes. In both algorithms, we recursively build a block Macaulay matrix $\boldsymbol{M}$ for increasing degree $d = 1, \ldots, 4$:

d	size	nullity	standard monomials
$d^* \to 1$	3×6	3	$z_1, z_2 \mid \lambda_1 z_1$
2	9×12	3	$z_1, z_2 \mid \lambda_1 z_1$
3	18×20	3	$z_1, z_2 \mid \lambda_1 z_1$
$d^* + d_g \to 4$	30×30	3	$z_1, z_2 \mid \lambda_1 z_1$

For this easy example, we notice via rank checks that the nullity of $\boldsymbol{M}$ has already stabilized for degree $d = 1$. Because we want to shift with a shift polynomial of degree $d_g = 3$, the degree d of $\boldsymbol{M}$ is *large enough* to accommodate the shift when $d \geq d^* + d_g = 4$. Via a singular value decomposition, we compute a numerical basis matrix $\boldsymbol{Z} \in \mathbb{C}^{30 \times 3}$ of its null space. The first three rows of $\boldsymbol{Z}$, which correspond to the variables z_1, z_2, and $\lambda_1 z_1$, are linearly independent (we obtain this information via row-wise rank checks of

$\boldsymbol{Z}$ from top to bottom) and correspond to the standard monomials. As the nullity is 3, there are no solutions at infinity. The row selection matrix $\boldsymbol{S}_1 \in \mathbb{R}^{3\times 30}$ selects these three linearly independent rows of $\boldsymbol{Z}$, and the row combination matrix $\boldsymbol{S}_g \in \mathbb{R}^{3\times 30}$ selects the rows that correspond to the monomials hit by shifting these standard monomials with $g(\lambda_1, \lambda_2) = 4\lambda_2^3$, namely the 19th ($\lambda_2^3 z_1$), 20th ($\lambda_2^3 z_2$), and 27th ($\lambda_1\lambda_2^3 z_1$) row:

$$\boldsymbol{S}_1 = \begin{array}{c} \begin{matrix} 1 & 2 & 3 & 4 & & 30 \end{matrix} \\ \begin{bmatrix} 1 & 0 & 0 & 0 & \cdots & 0 \\ 0 & 1 & 0 & 0 & \cdots & 0 \\ 0 & 0 & 1 & 0 & \cdots & 0 \end{bmatrix} \end{array} \text{ and}$$

$$\boldsymbol{S}_g = \begin{array}{c} \begin{matrix} 1 & & 18 & 19 & 20 & 21 & & 26 & 27 & 28 & 29 & 30 \end{matrix} \\ \begin{bmatrix} 0 & \cdots & 0 & 4 & 0 & 0 & \cdots & 0 & 0 & 0 & 0 & 0 \\ 0 & \cdots & 0 & 0 & 4 & 0 & \cdots & 0 & 0 & 0 & 0 & 0 \\ 0 & \cdots & 0 & 0 & 0 & 0 & \cdots & 0 & 4 & 0 & 0 & 0 \end{bmatrix} \end{array}.$$

After constructing $\boldsymbol{S}_1$ and $\boldsymbol{S}_g$, we set up the GEP in (7), and we compute the diagonal matrix $\boldsymbol{D}_g$ that contains the evaluation of the shift polynomial $g(\lambda_1, \lambda_2) = 4\lambda_2^3$ in the different solutions and the non-singular transformation matrix $\boldsymbol{T}$ that leads to the block Vandermonde basis matrix $\boldsymbol{V} = \boldsymbol{Z}\boldsymbol{T}$, from which we can retrieve the $m_b = m_a = 3$ affine solutions:

$$\boldsymbol{D}_g = \begin{bmatrix} 4\,\lambda_2^3\big|_{(1)} & 0 & 0 \\ 0 & 4\,\lambda_2^3\big|_{(2)} & 0 \\ 0 & 0 & 4\,\lambda_2^3\big|_{(3)} \end{bmatrix} \text{ and } \boldsymbol{V} = \left[\begin{array}{ccc} \boldsymbol{z}|_{(1)} & \boldsymbol{z}|_{(2)} & \boldsymbol{z}|_{(3)} \\ \hline (\lambda_1\boldsymbol{z})|_{(1)} & (\lambda_1\boldsymbol{z})|_{(2)} & (\lambda_1\boldsymbol{z})|_{(3)} \\ (\lambda_2\boldsymbol{z})|_{(1)} & (\lambda_2\boldsymbol{z})|_{(2)} & (\lambda_2\boldsymbol{z})|_{(3)} \\ \hline (\lambda_1^2\boldsymbol{z})|_{(1)} & (\lambda_1^2\boldsymbol{z})|_{(2)} & (\lambda_1^2\boldsymbol{z})|_{(3)} \\ \vdots & \vdots & \vdots \end{array}\right].$$

When we repeat this numerical example via the column space based approach, we start by identifying the linearly dependent columns (from right to left) of $\boldsymbol{M}$. We find that the first three columns are linearly dependent on the other columns (from right to left) and correspond to the standard monomials. We build the inverted row combination matrix $\boldsymbol{P}^{-1} \in \mathbb{R}^{30\times 30}$ as in Section 5.2 ($\boldsymbol{I}_s \in \mathbb{N}^{s\times s}$ is the identity matrix):

$$\boldsymbol{P} = \begin{bmatrix} \boldsymbol{I}_3 & \boldsymbol{0} & \boldsymbol{0} & \boldsymbol{0} & \boldsymbol{0} & \boldsymbol{0} \\ \boldsymbol{0} & \boldsymbol{0} & 4\boldsymbol{I}_2 & \boldsymbol{0} & \boldsymbol{0} & \boldsymbol{0} \\ \boldsymbol{0} & \boldsymbol{0} & \boldsymbol{0} & \boldsymbol{0} & 4\boldsymbol{I}_1 & \boldsymbol{0} \\ \boldsymbol{0} & \boldsymbol{I}_{15} & \boldsymbol{0} & \boldsymbol{0} & \boldsymbol{0} & \boldsymbol{0} \\ \boldsymbol{0} & \boldsymbol{0} & \boldsymbol{0} & \boldsymbol{I}_6 & \boldsymbol{0} & \boldsymbol{0} \\ \boldsymbol{0} & \boldsymbol{0} & \boldsymbol{0} & \boldsymbol{0} & \boldsymbol{0} & \boldsymbol{I}_3 \end{bmatrix} \text{ and } \boldsymbol{P}^{-1} = \begin{bmatrix} \boldsymbol{I}_3 & \boldsymbol{0} & \boldsymbol{0} & \boldsymbol{0} & \boldsymbol{0} & \boldsymbol{0} \\ \boldsymbol{0} & \boldsymbol{0} & \boldsymbol{0} & \boldsymbol{I}_{15} & \boldsymbol{0} & \boldsymbol{0} \\ \boldsymbol{0} & \frac{1}{4}\boldsymbol{I}_2 & \boldsymbol{0} & \boldsymbol{0} & \boldsymbol{0} & \boldsymbol{0} \\ \boldsymbol{0} & \boldsymbol{0} & \boldsymbol{0} & \boldsymbol{0} & \boldsymbol{I}_6 & \boldsymbol{0} \\ \boldsymbol{0} & \boldsymbol{0} & \frac{1}{4}\boldsymbol{I}_1 & \boldsymbol{0} & \boldsymbol{0} & \boldsymbol{0} \\ \boldsymbol{0} & \boldsymbol{0} & \boldsymbol{0} & \boldsymbol{0} & \boldsymbol{0} & \boldsymbol{I}_3 \end{bmatrix},$$

where the first three rows of $\boldsymbol{P}$ select the linearly independent rows of $\boldsymbol{B}$, the next three rows of $\boldsymbol{P}$ create the linear combinations of rows of $\boldsymbol{C}$, and the remaining rows of $\boldsymbol{P}$ result in $\boldsymbol{D}$. We do not multiply $\boldsymbol{Z}$ by $\boldsymbol{P}$, but we use $\boldsymbol{P}^{-1}$ to rearrange the columns

Table 2
The numerical solutions (and residual errors) of Example 4 obtained via the column space based algorithm. The residual error is determined by substituting the numerical solution in the linear 2-EP and calculating the norm of the residual vector $\|\boldsymbol{e}\|_2 = \|\boldsymbol{\mathcal{M}}(\lambda_1^*, \lambda_2^*)\boldsymbol{z}^*\|_2$.

λ_1	λ_2	z_1	z_2	$\|e\|_2$
0.9338	−1.3750	0.7848	0.6197	2.8×10^{-14}
1.3683	0.0552	0.8623	−0.5065	6.0×10^{-15}
3.6026	−0.4183	0.7958	−0.6056	2.6×10^{-14}

of $\boldsymbol{M}$ into the matrices $\boldsymbol{N}_1$, $\boldsymbol{N}_2$, and $\boldsymbol{N}_3$ (since there are no solutions at infinity, we do not have a matrix $\boldsymbol{N}_4$). The backward (Q-less) QR-decomposition of $\boldsymbol{N} = \boldsymbol{M}\boldsymbol{P}^{-1}$ results in the matrices $\boldsymbol{R}_{33}$ and $\boldsymbol{R}_{34}$ of (13) (see Footnote 6 for the structure of $\boldsymbol{R}$ when the matrix $\boldsymbol{N}_4$ is absent). The GEP yields the matrices $\boldsymbol{D}_g$ and $\boldsymbol{H}$, from which we can again retrieve the three affine solutions of the linear 2-EP:

$$\boldsymbol{D}_g = \begin{bmatrix} 4\lambda_2^3\big|_{(1)} & 0 & 0 \\ 0 & 4\lambda_2^3\big|_{(2)} & 0 \\ 0 & 0 & 4\lambda_2^3\big|_{(3)} \end{bmatrix} \text{ and } \boldsymbol{H} = \begin{bmatrix} z_1\big|_{(1)} & z_1\big|_{(2)} & z_1\big|_{(3)} \\ z_2\big|_{(1)} & z_2\big|_{(2)} & z_2\big|_{(3)} \\ \lambda_1 z_1\big|_{(1)} & \lambda_1 z_1\big|_{(2)} & \lambda_1 z_1\big|_{(3)} \end{bmatrix}.$$

The residual error[7] of all solutions obtained via the column space based approach is smaller than 2.8×10^{-14} and the maximum absolute difference with the null space based approach is equal to 2.2×10^{-13}. Table 2 contains the numerical solutions (and residual errors) obtained via the column space based algorithm.

6.2. Linear three-parameter eigenvalue problem with shift issues

In the previous example, any shift polynomial with a power of λ_2 yields a perfectly reconstructable solution. But as mentioned in Remark 4, the situation is sometimes more difficult.

Example 9. Let us consider the following linear three-parameter eigenvalue problem (linear 3-EP)

$$(\boldsymbol{A}_{000} + \boldsymbol{A}_{100}\lambda_1 + \boldsymbol{A}_{010}\lambda_2 + \boldsymbol{A}_{001}\lambda_3)\,\boldsymbol{z} = \boldsymbol{0},$$

with four coefficient matrices $\boldsymbol{A}_{\boldsymbol{\omega}} \in \mathbb{R}^{4\times 2}$,

$$\boldsymbol{A}_{000} = \begin{bmatrix} 2 & 3 \\ 2 & 5 \\ 0 & 1 \\ 1 & 1 \end{bmatrix}, \boldsymbol{A}_{100} = \begin{bmatrix} 1 & 0 \\ 0 & 1 \\ 1 & 1 \\ 2 & 1 \end{bmatrix}, \boldsymbol{A}_{010} = \begin{bmatrix} 4 & 2 \\ 2 & 3 \\ 3 & 1 \\ 3 & 1 \end{bmatrix}, \text{ and } \boldsymbol{A}_{001} = \begin{bmatrix} 1 & 2 \\ 1 & 4 \\ 2 & 1 \\ 4 & 2 \end{bmatrix}.$$

[7] We calculate the residual error by substituting the computed eigentuples $(\lambda_1^*, \ldots, \lambda_n^*)$ and eigenvectors $\boldsymbol{z}^*$ in the MEP and determining the norm of the residual vector $\|\boldsymbol{e}\|_2 = \|\boldsymbol{\mathcal{M}}(\lambda_1^*, \ldots, \lambda_n^*)\,\boldsymbol{z}^*\|_2$. The maximum absolute difference corresponds to the maximum difference between all the corresponding affine eigenvalues $\left|\lambda_{i,\text{null}}^* - \lambda_{i,\text{column}}^*\right|$, for $i = 1, \ldots, m_a$.

Table 3
The numerical solutions (and residual errors) of Example 9 obtained via the column space based algorithm. The residual error is determined by substituting the numerical solution in the linear 3-EP and calculating the norm of the residual vector $\|\boldsymbol{e}\|_2 = \|\boldsymbol{\mathcal{M}}(\lambda_1^*, \lambda_2^*, \lambda_3^*)\boldsymbol{z}^*\|_2$.

λ_1	λ_2	λ_3	z_1	z_2	$\|e\|_2$
−0.8534	1.1686	−1.5469	−0.4647	0.8854	1.2×10^{-14}
2.8123	−0.6635	−1.2924	0.7251	0.6886	2.3×10^{-14}
−1.3941	0.3207	0.2656	−0.8886	0.4588	9.4×10^{-14}
0.1653	−2.0595	0.1933	−0.1236	−0.9923	1.5×10^{-15}

We start with a block Macaulay matrix $\boldsymbol{M} \in \mathbb{R}^{16\times 20}$ of degree $d = 2 > d^*$ (see Footnote 6 for the structure of $\boldsymbol{R}$ when $\boldsymbol{M}$ is not tall). When we check the columns of $\boldsymbol{M}$ from right to left, we observe that the first four columns (which correspond to the variables z_1, z_2, $\lambda_1 z_1$, and $\lambda_1 z_2$) are linearly dependent on the other columns. Thus, the matrix $\boldsymbol{H}$ contains references to the variables z_1, z_2, $\lambda_1 z_1$, and $\lambda_1 z_2$ evaluated in each of the affine solutions, but no references to λ_2 or λ_3. Hence, not one, but two shift polynomials (with references to λ_2 and λ_3) are required to find all the components of the solutions via the eigenvalues of two different GEPs. We shift in this numerical example with $g_1(\lambda_1, \lambda_2, \lambda_3) = \lambda_2$ and $g_2(\lambda_1, \lambda_2, \lambda_3) = \lambda_3$ to obtain also the two remaining eigenvalues in $\boldsymbol{D}_{g_1}$ and $\boldsymbol{D}_{g_2}$. As mentioned in Remark 3, a shift with a monomial results in a row permutation matrix $\boldsymbol{P}$, which we can implement via column selections: for the shift $g_1(\lambda_1, \lambda_2, \lambda_3) = \lambda_2$, the inverse row selection matrix $\boldsymbol{P}^{-1}$ gathers the first four columns in $\boldsymbol{N}_1$ (which are the columns that correspond to the affine standard monomials), the 5th ($\lambda_2 z_1$), 6th ($\lambda_2 z_2$), 11th ($\lambda_1\lambda_2 z_1$), and 12th ($\lambda_1\lambda_2 z_1$) column in $\boldsymbol{N}_2$ (which are the columns hit by the shift), and the remaining columns in $\boldsymbol{N}_3$ (a similar column selection exists for the shift $g_2(\lambda_1, \lambda_2, \lambda_3) = \lambda_3$). In order to match the different eigenvalues λ_2 and λ_3, we can use the matrix of eigenvectors $\boldsymbol{H}$ in both GEPs or work with the Schur decomposition [6,16]. Table 3 contains the solutions obtained via the column space based approach. The maximum residual error and maximum absolute difference with the null space based approach (both calculated as in the first numerical example[7]) are equal to 9.4×10^{-14} and 1.0×10^{-13}, respectively.

6.3. Volkmer's square two-parameter eigenvalue problem

In Example 6, we show how to transform the regular linear square 2-EP into a linear rectangular 2-EP. To demonstrate that our algorithms can also solve this transformed problem with overdetermined coefficient matrices (i.e., $k = 2l > l+n-1$), we solve (4) via the null space and column space based approach. A block Macaulay matrix $\boldsymbol{M} \in \mathbb{R}^{36\times 36}$ of degree $d = 2 > d^*$ suffices to compute the same eigenvalues as in [52]. Table 4 contains the results of the column space based algorithm (maximum residual error[7] is 2.7×10^{-13}), which are identical to the results of the null space based algorithm (maximum absolute difference[7] is 1.4×10^{-14}). Note that our results agree with the results obtained by the

Table 4
The numerical solutions (and residual errors) of Example 6 obtained via the column space based algorithm. The residual error is determined by substituting the numerical solution in the linear 2-EP and calculating the norm of the residual vector $\|\boldsymbol{e}\|_2 = \|\boldsymbol{\mathcal{M}}(\lambda_1^*, \lambda_2^*)\boldsymbol{z}^*\|_2$.

λ_1	λ_2	z_1	z_2	z_3	z_4	z_5	z_6	$\|e\|_2$
−5.0000	−5.0000	−0.4811	0.8333	0.0962	−0.1667	−0.0962	0.1667	2.7×10^{-13}
−1.0000	−3.0000	0.2611	−0.1508	0.2611	−0.1508	−0.7833	0.4523	1.4×10^{-13}
−4.1089	1.6171	0.2210	0.9726	0.0149	0.0655	0.0059	0.0258	1.2×10^{-14}
1.4422	−3.1410	0.1832	0.1457	0.3175	0.2525	0.6915	0.5499	1.1×10^{-13}
0.0000	0.0000	0.0000	0.0000	0.0000	1.0000	0.0000	0.0000	1.0×10^{-16}
0.0000	0.0000	0.0000	0.0000	0.0000	0.0000	0.0000	1.0000	1.0×10^{-16}

MultiParEig toolbox [42], which solves (3) via the QZ-algorithm and results in a maximum residual error of 6.3×10^{-14}.

6.4. Polynomial two-parameter eigenvalue problem with solutions at infinity

Next, we revisit the polynomial MEP with two parameters from Example 5 and use a shift polynomial $g(\lambda_1, \lambda_2) = \lambda_1$. We recursively build the block Macaulay matrix $\boldsymbol{M}$ for increasing degree $d = 2, \ldots, 5$:

	d	size	nullity	standard monomials
	2	3×12	9	$z_1, z_2 \mid \lambda_1 z_1, \lambda_1 z_2, \lambda_2 z_1, \lambda_2 z_2 \mid \lambda_1^2 z_1, \lambda_1^2 z_2, \lambda_1\lambda_2 z_1$
	3	9×20	11	$z_1, z_2 \mid \lambda_1 z_1, \lambda_1 z_2, \lambda_2 z_1, \lambda_2 z_2 \mid \lambda_1^2 z_1, \lambda_1^2 z_2, \lambda_1\lambda_2 z_1 \mid \lambda_1^3 z_1, \lambda_1^3 z_2$
$d^* \to$	4	18×30	12	$z_1, z_2 \mid \lambda_1 z_1, \lambda_1 z_2, \lambda_2 z_1, \lambda_2 z_2 \mid \lambda_1^2 z_1, \lambda_1^2 z_2, \lambda_1\lambda_2 z_1 \mid \lambda_1^3 z_1 \mid \lambda_1^4 z_1, \lambda_1^4 z_2$
$d^* + d_g \to$	5	30×42	12	$z_1, z_2 \mid \lambda_1 z_1, \lambda_1 z_2, \lambda_2 z_1, \lambda_2 z_2 \mid \lambda_1^2 z_1, \lambda_1^2 z_2, \lambda_1\lambda_2 z_1 \mid$ **gap** $\mid \lambda_1^4 z_1 \mid \lambda_1^5 z_1, \lambda_1^5 z_2$

A degree $d = 5$ block Macaulay matrix $\boldsymbol{M}$ suffices to solve this MEP via both the null space and column space based approach. In the null space based algorithm, we need to compute a numerical basis matrix $\boldsymbol{Z} \in \mathbb{C}^{42\times 12}$ of the null space (since we have $m_b = 12$ solutions) and determine the gap via row-wise rank checks from top to bottom. The gap indicates that this problem has $m_a = 9$ affine solutions and $m_\infty = 3$ solutions at infinity. At this degree, the linearly independent rows related to the affine standard monomials have stabilized. We notice an analogue behavior in the column space of $\boldsymbol{M}$. However, because of the backward (Q-less) QR-decomposition, we do not need to deflate the solutions at infinity via a column compression. Note that for degree $d = 5$ the block Macaulay matrix is not yet tall, i.e., $p < q$ (see Footnote 6 for the structure of $\boldsymbol{R}$ when $p = q - m_b < q - m_a$). We can alleviate this problem by using a larger degree d or by removing the linearly dependent columns in $\boldsymbol{N}_4$. We choose in this numerical example the latter option and remove the 21st ($\lambda_1^4 z_1$), 31st ($\lambda_1^5 z_1$), and 32nd ($\lambda_1^5 z_2$) column from $\boldsymbol{M}$ when splitting into $\boldsymbol{N}_1$, $\boldsymbol{N}_2$, $\boldsymbol{N}_3$, and $\boldsymbol{N}_4$. Algorithm 2 obtains the affine solution of Table 5. The maximum residual error of the column space based algorithm is 4.8×10^{-13}, while the maximum absolute difference with the null space based results is equal to 1.7×10^{-12} (both calculated as in the first numerical example[7]).

Table 5
The affine numerical solutions (and residual errors) of Example 5 obtained via the column space based algorithm. The residual error is determined by substituting the numerical solution in the polynomial 2-EP and calculating the norm of the residual vector $\|\boldsymbol{e}\|_2 = \|\boldsymbol{\mathcal{M}}(\lambda_1^*, \lambda_2^*)\boldsymbol{z}^*\|_2$.

λ_1	λ_2	z_1	z_2	$\|e\|_2$
$1.4027 \pm 0.3941i$	$-1.3835 \mp 0.8431i$	$0.4676 \mp 0.5024i$	$-0.6678 \pm 0.2881i$	5.1×10^{-14}
$-0.9699 \pm 0.7168i$	$-0.1113 \pm 0.5741i$	0.4140 ∓ 0.5713	$0.2080 \pm 0.6775i$	1.1×10^{-14}
$0.8543 + 0.0000i$	$-0.9341 + 0.0000i$	$-0.7644 + 0.0000i$	$0.6448 + 0.0000i$	2.8×10^{-15}
$0.2737 + 0.0751i$	$-0.1917 \mp 0.2408i$	$0.8272 \pm 0.0000i$	$-0.5617 \mp 0.0171i$	1.0×10^{-14}
$-0.4497 \pm 0.0662i$	$0.6094 \mp 1.0534i$	$0.1726 \mp 0.5241i$	$0.4176 \pm 0.7219i$	7.6×10^{-14}

6.5. System identification problem

Finally, we consider the identification of the globally optimal parameters of an ARMA model via the MEP methodology described by Vermeersch and De Moor [50]. We consider a first-order ARMA(1, 1) model, which combines a regression of the observed output variable $y_k \in \mathbb{R}$ on its own lagged value y_{k-1} with a linear combination of unobserved, latent inputs l_k and $l_{k-1} \in \mathbb{R}$ [11]:

$$y_k + \alpha y_{k-1} = l_k + \gamma l_{k-1}, \tag{14}$$

where the weighting factors α and γ are the model parameters of this ARMA model. For a given series of N output samples $\boldsymbol{y} \in \mathbb{R}^{N\times 1}$, we search the model parameters that minimize the sum of squares of the latent inputs $\sigma^2 = \|\boldsymbol{l}\|_2^2$, subject to the ARMA(1, 1) model structure of (14), which corresponds to

$$\min_{\boldsymbol{l},\alpha,\gamma} \|\boldsymbol{l}\|_2^2$$
$$\text{subject to } y_k + \alpha y_{k-1} = l_k + \gamma l_{k-1},$$

for all data points y_k $(k = 2, \ldots, N)$ in the given series of output samples $\boldsymbol{y}$. Vermeersch and De Moor [50] have shown that the globally optimal solution to this identification problem is given by a quadratic two-parameter eigenvalue problem $\left(\boldsymbol{A}_{00} + \boldsymbol{A}_{10}\alpha + \boldsymbol{A}_{01}\gamma + \boldsymbol{A}_{02}\gamma^2\right)\boldsymbol{z} = \boldsymbol{0}$. The exact construction of the $(3N-1)\times(3N-2)$ coefficient matrices $\boldsymbol{A}_{\boldsymbol{\omega}}$ can be found in [50]. We apply this approach on a sequence of $N = 7$ output samples (without any a priori assumptions)

$$\boldsymbol{y} = \begin{bmatrix} 1.5000 \\ -0.3591 \\ 0.1129 \\ 0.5449 \\ -0.0790 \\ 0.1143 \\ 0.1368 \end{bmatrix}. \tag{15}$$

We now use both block Macaulay matrix algorithms to solve the quadratic two-parameter eigenvalue problem (with 20×19 coefficient matrices $\boldsymbol{A}_{\boldsymbol{\omega}}$) that yields the

Table 6
The identified real parameters α and γ of the ARMA$(1,1)$ model given by the data in (15), computed via the column space based algorithm. The value of the objective function σ^2 in the identified minimum is smaller than in the saddle points.

Stationary point	α	γ	σ^2
Saddle point	-0.1172	-0.7597	0.5750
Saddle point	0.1136	0.8416	0.4699
Minimum	0.2097	0.1611	0.3531

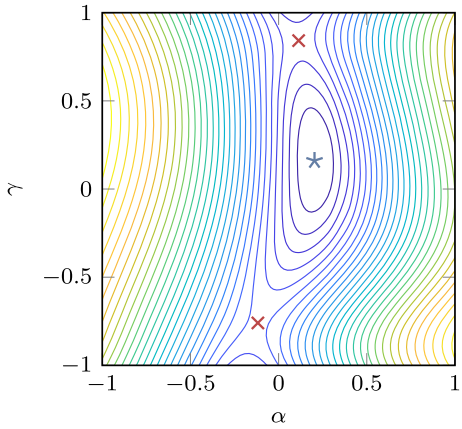

Fig. 4. The contour plot of the objective function of the ARMA$(1,1)$ model given by the data in (15) for the model parameters α and γ in the unit interval $[-1,1]$. The value of the objective function σ^2 in the minimum ($\star$) identified via the column space based approach is smaller than in the saddle points ($\times$).

optimal model parameters. The solution set of this problem is positive-dimensional at infinity, which means that the nullity of the block Macaulay matrix does not stabilize (there are an infinite number of solutions). Instead of checking the nullity of the block Macaulay matrix for a growing degree d, we monitor the standard monomials and look for the emergence of a gap zone, which we observe for a degree $d = 37$ block Macaulay matrix with size 13320×14079. Afterwards, a column compression (null space based approach) or a backward (Q-less) QR-decomposition (column space based approach) deflates the positive-dimensional solution set at infinity and we find $m_a = 77$ affine solutions for the MEP. Only three solutions are real, and hence interesting in this practical setting: we find one minimum and two saddle points (see Table 6). When we compare this identified minimum with a visualization (Fig. 4) of the objective function σ^2, we observe that we indeed have a global minimum within the unit domain $[-1,1] \times [-1,1]$. One immediately notices that the matrices involved in this identification problem quickly grow much larger than in our previous numerical examples. Realistic problems fuel the search for more efficient implementations that exploit the sparsity and structure of the block Macaulay matrix.

7. Conclusion and future work

In this paper, we exploited the complementarity between the null space and column space of the block Macaulay matrix to propose a new algorithm that considers the column space of the block Macaulay matrix. Contrary to the existing null space based approach, this column space based algorithm does not require an explicit computation of a numerical basis matrix of the null space, but considers the data in the columns of the block Macaulay matrix directly and removes the influence of the solutions at infinity implicitly via a backward (Q-less) QR-decomposition. We also provided several numerical examples to illustrate both block Macaulay matrix algorithms and to test our new column space based approach.

Our last numerical example, the globally optimal least-squares identification of an ARMA model, has fueled several new research ideas. When the coefficient matrices grow, the computational complexity of both the null space and column space based algorithm increases rapidly. In particular the rank checks to determine the linearly independent rows of the basis matrix or the linearly dependent columns of the block Macaulay matrix are computationally expensive. The backward (Q-less) QR-decomposition, which constitutes the core of the column space based approach, has created several algorithmic opportunities. We want to improve the column space based algorithm by exploiting the sparsity and structure of the block Macaulay matrix, by considering block columns instead of columns (i.e., by taking fully advantage of the backward block multi-shift-invariance), by looking into rank-revealing QR-decompositions, and by developing recursive techniques. Furthermore, the complementarity between both fundamental subspaces may even yield more useful properties in the column space. Together with a better understanding of MEPs, these advances will give us the machinery to tackle much larger problems in the future.

Declaration of competing interest

The authors declare that they have no known competing financial interests or personal relationships that could have appeared to influence the work reported in this paper.

Acknowledgements

The authors want to thank Bob Vergauwen, Katrien De Cock, and Philippe Dreesen for their helpful insights and constructive feedback.

Appendix A. Backward scalar/block single/multi-shift-invariant subspaces

The algorithms in this paper strongly rely on the concept of backward (block multi-) shift-invariance. Shift-invariance of a subspace is usually defined for infinite matrices,

i.e., operators [26]. De Cock and De Moor [19] have adapted in their paper the definition of backward scalar/block single/multi-shift-invariance to finite dimensional subspaces.[8]

Definition 5 *(Backward scalar single-shift-invariance).* Let $\mathcal{R}(\boldsymbol{G})$ be the range of a matrix $\boldsymbol{G} \in \mathbb{C}^{m\times n}$ with full column rank. $\mathcal{R}(\boldsymbol{G})$ is **backward scalar single-shift-invariant** if and only if

$$\mathcal{R}\left(\overline{\boldsymbol{G}}\right) \subseteq \mathcal{R}\left(\underline{\boldsymbol{G}}\right),$$

where $\overline{\boldsymbol{G}}$ and $\underline{\boldsymbol{G}}$ (with full column rank) are the matrix $\boldsymbol{G}$ without its first and last row, respectively.

The backward scalar single-shift-invariance of $\mathcal{R}(\boldsymbol{G})$ can also be expressed as

$$\exists \boldsymbol{\Gamma} \in \mathbb{C}^{n\times n} : \underline{\boldsymbol{G}}\boldsymbol{\Gamma} = \overline{\boldsymbol{G}},$$

where $\mathcal{R}\left(\overline{\boldsymbol{G}}\right) = \mathcal{R}\left(\underline{\boldsymbol{G}}\right)$ if $\boldsymbol{\Gamma}$ is non-singular (and otherwise $\mathcal{R}\left(\overline{\boldsymbol{G}}\right) \subsetneq \mathcal{R}\left(\underline{\boldsymbol{G}}\right)$). We can rewrite these row selections via row selection matrices $\boldsymbol{S}_1$ and $\boldsymbol{S}_2$, similar to the mathematical formulation in other parts of this paper. The property above can then be expressed as

$$\exists \boldsymbol{\Gamma} \in \mathbb{C}^{n\times n} : (\boldsymbol{S}_1\boldsymbol{G})\,\boldsymbol{\Gamma} = (\boldsymbol{S}_2\boldsymbol{G}), \tag{A.1}$$

where $\boldsymbol{S}_1$ and $\boldsymbol{S}_2$ select all the rows of the matrix $\boldsymbol{G}$ except the last one and the first one, respectively. Note that shift-invariance is a property of the vector space, and not of the specific basis matrix of this vector space. If we consider a second basis matrix $\boldsymbol{H} \in \mathbb{C}^{m\times n}$, then there exists a basis transformation via a non-singular matrix $\boldsymbol{T} \in \mathbb{C}^{n\times n}$, such that $\boldsymbol{G} = \boldsymbol{H}\boldsymbol{T}$. Consequently, we can rewrite (A.1) as

$$(\boldsymbol{S}_1\boldsymbol{H})\,\boldsymbol{\Lambda} = (\boldsymbol{S}_2\boldsymbol{H}), \quad \text{with } \boldsymbol{\Lambda} = \boldsymbol{T}\boldsymbol{\Gamma}\boldsymbol{T}^{-1}.$$

Clearly, the matrices $\boldsymbol{\Gamma}$ and $\boldsymbol{\Lambda}$ are similar, and hence have the same spectrum. This property allows us to interpret the basis matrices of backward shift-invariant column spaces as observability matrices of multidimensional systems. In that regard, we can see the null space based solution approach, where we search for the spectrum of $\boldsymbol{\Gamma}$ (or $\boldsymbol{\Lambda}$), as a multidimensional realization problem. Then, the full rank condition of $\boldsymbol{G}$ is equivalent with the system being observable and the full rank condition of $\underline{\boldsymbol{G}}$ is the partial realization condition, required for a unique solution [19,25].

[8] Note that sometimes ambiguity arises when considering the shift operator. In this paper, we adopt the convention of Garcia et al. [26], and we define the backward shift operator as $\mathcal{S}\{f(z)\} = \frac{f(z)-f(0)}{z}$, or, in terms of Taylor coefficients $\{a_i\}_{i\geq 0}$ of $f(z)$, as $\mathcal{S}\{(a_0, a_1, \ldots)\} = (a_1, a_2, \ldots)$.

Example 10 ***(Backward scalar single-shift-invariance).*** When we consider a univariate Vandermonde matrix $\boldsymbol{V}_U \in \mathbb{C}^{(d+1)\times n}$ (with n distinct variables and a degree d), we observe an example of this shift-invariance[9]:

$$\underbrace{\begin{bmatrix} 1 & \cdots & 1 \\ \alpha_1 & \cdots & \alpha_n \\ \vdots & & \vdots \\ \alpha_1^{d-1} & \cdots & \alpha_n^{d-1} \end{bmatrix}}_{\boldsymbol{S}_1\boldsymbol{V}_U} \underbrace{\begin{bmatrix} \alpha_1 & \cdots & 0 \\ \vdots & \ddots & \vdots \\ 0 & \cdots & \alpha_n \end{bmatrix}}_{\boldsymbol{\Gamma}} = \underbrace{\begin{bmatrix} \alpha_1 & \cdots & \alpha_n \\ \vdots & & \vdots \\ \alpha_1^{d-1} & \cdots & \alpha_n^{d-1} \\ \alpha_1^{d} & \cdots & \alpha_n^{d} \end{bmatrix}}_{\boldsymbol{S}_2\boldsymbol{V}_U}.$$

Definition 5 covers backward scalar single-shift-invariance: *scalar* meaning that we shift row-wise and *single-shift* meaning that only one shift is possible in the subspace. We can extend this definition and consider *backward block single-shift-invariant*, *backward scalar multi-shift-invariant*, and *backward block multi-shift-invariant subspaces*.

Example 11 ***(Backward block single-shift-invariance).*** While the column space of the matrix $\boldsymbol{V}_U$ is backward scalar single-shift-invariant, some subspaces are backward block single-shift-invariant, which means that we can shift entire block rows of the basis matrix, e.g., $\mathcal{R}(\boldsymbol{S}_1\boldsymbol{G}) \subseteq \mathcal{R}(\boldsymbol{S}_2\boldsymbol{G})$, where the row selection matrices $\boldsymbol{S}_1$ and $\boldsymbol{S}_2$ select the entire matrix $\boldsymbol{G}$ without the first and last block row, respectively. A block univariate Vandermonde matrix $\boldsymbol{V}_B \in \mathbb{C}^{(d+1)s\times n}$ (with a vector $\boldsymbol{z}_i \in \mathbb{C}^{s\times 1}, i = 1, \ldots, n$) exhibits this property:

$$\underbrace{\begin{bmatrix} \boldsymbol{z}_1 & \cdots & \boldsymbol{z}_n \\ \alpha_1\boldsymbol{z}_1 & \cdots & \alpha_n\boldsymbol{z}_n \\ \vdots & & \vdots \\ \alpha_1^{d-1}\boldsymbol{z}_1 & \cdots & \alpha_n^{d-1}\boldsymbol{z}_n \end{bmatrix}}_{\boldsymbol{S}_1\boldsymbol{V}_B} \underbrace{\begin{bmatrix} \alpha_1 & \cdots & 0 \\ \vdots & \ddots & \vdots \\ 0 & \cdots & \alpha_n \end{bmatrix}}_{\boldsymbol{\Gamma}} = \underbrace{\begin{bmatrix} \alpha_1\boldsymbol{z}_1 & \cdots & \alpha_n\boldsymbol{z}_n \\ \vdots & & \vdots \\ \alpha_1^{d-1}\boldsymbol{z}_1 & \cdots & \alpha_n^{d-1}\boldsymbol{z}_n \\ \alpha_1^{d}\boldsymbol{z}_1 & \cdots & \alpha_n^{d}\boldsymbol{z}_n \end{bmatrix}}_{\boldsymbol{S}_2\boldsymbol{V}_B}.$$

Example 12 ***(Backward scalar multi-shift-invariance).*** In the previous examples, we only consider shifts with one variable. Now, we look at subspaces with multiple shifts and consider the backward scalar multi-shift-invariance of a subspace. An example is the bivariate Vandermonde matrix $\boldsymbol{V}_M \in \mathbb{C}^{(2d+1)\times n}$,

$$\boldsymbol{V}_M = \begin{bmatrix} 1 & \cdots & 1 \\ \alpha_1 & \cdots & \alpha_n \\ \beta_1 & \cdots & \beta_n \\ \alpha_1^2 & \cdots & \alpha_n^2 \\ \vdots & & \vdots \\ \beta_1^d & \cdots & \beta_n^d \end{bmatrix},$$

[9] In this appendix, we abuse the notation for readability: $\alpha_j = \alpha|_{(j)}$, $\beta_j = \beta|_{(j)}$, and $\boldsymbol{z}_j = \boldsymbol{z}|_{(j)}$ $(j = 1, \ldots, n)$.

which can be shifted by both variables α and β. As an example, we shift the first three rows of $\boldsymbol{V}_M$:

$$\underbrace{\begin{bmatrix} 1 & \cdots & 1 \\ \alpha_1 & \cdots & \alpha_n \\ \beta_1 & \cdots & \beta_n \end{bmatrix}}_{\boldsymbol{S}_1\boldsymbol{V}_M} \underbrace{\begin{bmatrix} \alpha_1 & \cdots & 0 \\ \vdots & \ddots & \vdots \\ 0 & \cdots & \alpha_n \end{bmatrix}}_{\boldsymbol{\Gamma}_\alpha} = \underbrace{\begin{bmatrix} \alpha_1 & \cdots & \alpha_n \\ \alpha_1^2 & \cdots & \alpha_n^2 \\ \alpha_1\beta_1 & \cdots & \alpha_n\beta_n \end{bmatrix}}_{\boldsymbol{S}_2\boldsymbol{V}_M}$$

$$\underbrace{\begin{bmatrix} 1 & \cdots & 1 \\ \alpha_1 & \cdots & \alpha_n \\ \beta_1 & \cdots & \beta_n \end{bmatrix}}_{\boldsymbol{S}_1\boldsymbol{V}_M} \underbrace{\begin{bmatrix} \beta_1 & \cdots & 0 \\ \vdots & \ddots & \vdots \\ 0 & \cdots & \beta_n \end{bmatrix}}_{\boldsymbol{\Gamma}_\beta} = \underbrace{\begin{bmatrix} \beta_1 & \cdots & \beta_n \\ \alpha_1\beta_1 & \cdots & \alpha_n\beta_n \\ \beta_1^2 & \cdots & \beta_n^2 \end{bmatrix}}_{\boldsymbol{S}_3\boldsymbol{V}_M},$$

where the row selection matrices $\boldsymbol{S}_2$ and $\boldsymbol{S}_3$ select the rows of the bivariate Vandermonde matrix after a shift of the first three rows (the matrix $\boldsymbol{S}_1$) by α (the matrix $\boldsymbol{\Gamma}_\alpha$) and by β (the matrix $\boldsymbol{\Gamma}_\beta$), respectively.

Example 13 ***(Backward block multi-shift-invariance).*** Backward block multi-shift-invariance is a natural extension of the previous types of shift-invariant subspaces. This property appears multiple times in this paper, since the (affine) null space of the block Macaulay matrix is backward block multi-shift-invariant. As an example, we shift the first three block rows of the block multivariate Vandermonde matrix (compare to (5) with $\boldsymbol{\lambda} = (\alpha, \beta)$):

$$\underbrace{\begin{bmatrix} \boldsymbol{z}_1 & \cdots & \boldsymbol{z}_n \\ \alpha_1\boldsymbol{z}_1 & \cdots & \alpha_n\boldsymbol{z}_n \\ \beta_1\boldsymbol{z}_1 & \cdots & \beta_n\boldsymbol{z}_n \end{bmatrix}}_{\boldsymbol{S}_1\boldsymbol{V}} \underbrace{\begin{bmatrix} \alpha_1 & \cdots & 0 \\ \vdots & \ddots & \vdots \\ 0 & \cdots & \alpha_n \end{bmatrix}}_{\boldsymbol{\Gamma}_\alpha} = \underbrace{\begin{bmatrix} \alpha_1\boldsymbol{z}_1 & \cdots & \alpha_n\boldsymbol{z}_1 \\ \alpha_1^2\boldsymbol{z}_1 & \cdots & \alpha_n^2\boldsymbol{z}_n \\ \alpha_1\beta_1\boldsymbol{z}_1 & \cdots & \alpha_n\beta_n\boldsymbol{z}_n \end{bmatrix}}_{\boldsymbol{S}_2\boldsymbol{V}}$$

$$\underbrace{\begin{bmatrix} \boldsymbol{z}_1 & \cdots & \boldsymbol{z}_n \\ \alpha_1\boldsymbol{z}_1 & \cdots & \alpha_n\boldsymbol{z}_n \\ \beta_1\boldsymbol{z}_1 & \cdots & \beta_n\boldsymbol{z}_n \end{bmatrix}}_{\boldsymbol{S}_1\boldsymbol{V}} \underbrace{\begin{bmatrix} \beta_1 & \cdots & 0 \\ \vdots & \ddots & \vdots \\ 0 & \cdots & \beta_n \end{bmatrix}}_{\boldsymbol{\Gamma}_\beta} = \underbrace{\begin{bmatrix} \beta_1\boldsymbol{z}_1 & \cdots & \beta_n\boldsymbol{z}_n \\ \alpha_1\beta_1\boldsymbol{z}_1 & \cdots & \alpha_n\beta_n\boldsymbol{z}_n \\ \beta_1^2\boldsymbol{z}_1 & \cdots & \beta_n^2\boldsymbol{z}_n \end{bmatrix}}_{\boldsymbol{S}_3\boldsymbol{V}}.$$

References

[1] F.V. Atkinson, Multiparameter spectral theory, Bull. Am. Math. Soc. 74 (1968) 1–27.
[2] F.V. Atkinson, Multiparameter Eigenvalue Problems, Mathematics in Science and Engineering, vol. 82, Academic Press, New York, NY, USA, 1972.
[3] F.V. Atkinson, A.B. Mingarelli, Multiparameter Eigenvalue Problems: Sturm–Liouville Theory, CRC Press, Boca Raton, FL, USA, 2010.
[4] K. Batselier, A Numerical Linear Algebra Framework for Solving Problems with Multivariate Polynomials, Ph.D. thesis, KU Leuven, Leuven, Belgium, 2013.
[5] K. Batselier, P. Dreesen, B. De Moor, The geometry of multivariate polynomial division and elimination, SIAM J. Matrix Anal. Appl. 34 (2013) 102–125.
[6] K. Batselier, P. Dreesen, B. De Moor, On the null spaces of the Macaulay matrix, Linear Algebra Appl. 460 (2014) 259–289.

[7] E.K. Blum, A.F. Chang, A numerical method for the solution of the double eigenvalue problem, IMA J. Appl. Math. 22 (1978) 29–42.
[8] E.K. Blum, A.R. Curtis, A convergent gradient method for matrix eigenvector-eigentuple problems, Numer. Math. 31 (1978) 247–263.
[9] E.K. Blum, P.B. Geltner, Numerical solution of eigentuple-eigenvector problems in Hilbert spaces by a gradient method, Numer. Math. 31 (1978) 231–246.
[10] Z. Bohte, Numerical solution of some two-parameter eigenvalue problems, in: Anton Kuhelj Memorial Volume, Slovenian Academy of Science and Art, Ljubljana, Slovenia, 1982, pp. 17–28.
[11] G.E.P. Box, G.M. Jenkins, revised ed., Time Series Analysis: Forecasting and Control. Holden-Day Series in Time Series Analysis., Holden Day, Oakland, CA, USA, 1976.
[12] P.J. Browne, B.D. Sleeman, A numerical technique for multiparameter eigenvalue problems, IMA J. Numer. Anal. 2 (1982) 451–457.
[13] R.D. Carmichael, Boundary value and expansion problems: algebraic basis of the theory, Am. J. Math. 43 (1921) 69–101.
[14] R.D. Carmichael, Boundary value and expansion problems: formulation of various transcedental problems, Am. J. Math. 43 (1921) 232–270.
[15] R.D. Carmichael, Boundary value and expansion problems: oscillation, comparison and expansion theorems, Am. J. Math. 44 (1922) 129–152.
[16] R.M. Corless, G.M. Patrizia, B.M. Trager, A reordered Schur factorization method for zero-dimensional polynomial systems with multiple roots, in: Proc. of the 1997 Symposium on Symbolic and Algebraic Computation (ISSAC), Maui, HI, USA, 1997, pp. 133–140.
[17] D.A. Cox, J.B. Little, D. O'Shea, Ideals, Varieties, and Algorithms, 3rd ed., Undergraduate Texts in Mathematics, Springer, New York, NY, USA, 2007.
[18] B.H. Dayton, T.Y. Li, Z. Zeng, Multiple zeros of nonlinear systems, Math. Comput. 80 (2011) 2143–2168.
[19] K. De Cock, B. De Moor, Multiparameter eigenvalue problems and shift-invariance, IFAC-PapersOnLine 54 (2021) 159–165. Part of special issue: 24th International Symposium on Mathematical Theory of Networks and Systems (MTNS).
[20] B. De Moor, Least squares realization of LTI models is an eigenvalue problem, in: Proc. of the 18th European Control Conference (ECC), Naples, Italy, 2019, pp. 2270–2275.
[21] B. De Moor, Least squares optimal realisation of autonomous LTI systems is an eigenvalue problem, Commun. Inf. Syst. 20 (2020) 163–207.
[22] B. Dong, B. Yu, Y. Yu, A homotopy method for finding all solutions of a multiparameter eigenvalue problem, SIAM J. Matrix Anal. Appl. 37 (2016) 550–571.
[23] P. Dreesen, Back to the Roots: Polynomial System Solving Using Linear Algebra, Ph.D. thesis, KU Leuven, Leuven, Belgium, 2013.
[24] P. Dreesen, K. Batselier, B. De Moor, Back to the roots: polynomial system solving, linear algebra, systems theory, in: Proc. of the 16th IFAC Symposium on System Identification, Brussels, Belgium, 2012, pp. 1203–1208.
[25] P. Dreesen, K. Batselier, B. De Moor, Multidimensional realisation theory and polynomial system solving, Int. J. Control 91 (2018) 2692–2704.
[26] S.R. Garcia, J. Mashreghi, W.T. Ross, Introduction to Model Spaces and Their Operators, Cambridge Studies in Advanced Mathematics, Cambridge University Press, Cambridge, UK, 2016.
[27] G.H. Golub, C.F. Van Loan, Matrix Computations, 4th ed., Johns Hopkins University Press, Baltimore, MD, USA, 2013.
[28] N.J. Higham, S.D. Mackey, F. Tisseur, The conditioning of linearizations of matrix polynomials, SIAM J. Matrix Anal. Appl. 28 (2006) 1005–1028.
[29] D. Hilbert, Grundzüge einer allgemeinen Theorie der linearen Integralgleichungen (erste Mitteilung), Nachrichten von der Königlichen Gesellschaft der Wissenschaften zu Göttingen, 1904, pp. 49–91.
[30] M.E. Hochstenbach, T. Košir, B. Plestenjak, A Jacobi–Davidson type method for the two-parameter eigenvalue problem, SIAM J. Matrix Anal. Appl. 26 (2004) 477–497.
[31] M.E. Hochstenbach, K. Meerbergen, E. Mengi, B. Plestenjak, Subspace methods for three-parameter eigenvalue problems, Numer. Linear Algebra Appl. 26 (2019) 1–22.
[32] M.E. Hochstenbach, A. Muhič, B. Plestenjak, On linearizations of the quadratic two-parameter eigenvalue problem, Linear Algebra Appl. 436 (2012) 2725–2743.
[33] M.E. Hochstenbach, B. Plestenjak, A Jacobi–Davidson type method for a right definite two-parameter eigenvalue problem, SIAM J. Matrix Anal. Appl. 24 (2002) 392–410.
[34] M.E. Hochstenbach, B. Plestenjak, Harmonic Rayleigh–Ritz extraction for the multiparameter eigenvalue problem, Electron. Trans. Numer. Anal. 29 (2008) 81–96.

[35] X. Ji, Numerical solution of joint eigenpairs of a family of commutative matrices, Appl. Math. Lett. 4 (1991) 57–60.
[36] T. Košir, B. Plestenjak, On the Singular Two-Parameter Eigenvalue Problem II, Technical Report, University of Ljubljana, Ljubljana, Slovenia, 2021.
[37] F.S. Macaulay, Some formulae in elimination, Proc. Lond. Math. Soc. 1 (1902) 3–27.
[38] F.S. Macaulay, The Algebraic Theory of Modular Systems, Cambridge Tracts in Mathematics and Mathematical Physics, vol. 19, Cambridge University Press, London, UK, 1916.
[39] M.H. Möller, H.J. Stetter, Multivariate polynomial equations with multiple zeros solved by matrix eigenproblems, Numer. Math. 70 (1995) 311–329.
[40] A. Muhič, B. Plestenjak, On the singular two-parameter eigenvalue problem, Electron. J. Linear Algebra 18 (2009) 420–437.
[41] B. Plestenjak, A continuation method for a right definite two-parameter eigenvalue problem, SIAM J. Matrix Anal. Appl. 21 (2000) 1163–1184.
[42] B. Plestenjak, Multipareig: toolbox for multiparameter eigenvalue problems, https://mathworks.com/matlabcentral/fileexchange/47844-multipareig, 2018 (Visited on December 14, 2021).
[43] B. Plestenjak, C.I. Gheorghiu, M.E. Hochstenbach, Spectral collocation for multiparameter eigenvalue problems arising from separable boundary value problems, J. Comput. Phys. 298 (2015) 585–601.
[44] J.I. Rodriguez, J.H. Du, Y. You, L.H. Lim, Fiber product homotopy method for multiparameter eigenvalue problems, Numer. Math. 148 (2021) 853–888.
[45] K. Ruymbeek, K. Meerbergen, W. Michiels, Subspace method for multiparameter-eigenvalue problems based on tensor-train representations, Numer. Linear Algebra Appl. e2439 (2022) 1–20.
[46] B. Shapiro, M. Shapiro, On eigenvalues of rectangular matrices, Proc. Steklov Inst. Math. 267 (2009) 248–255.
[47] B.D. Sleeman, Multiparameter spectral theory and separation of variables, J. Phys. A, Math. Theor. 41 (2007) 1–20.
[48] T. Slivnik, G. Tomšič, A numerical method for the solution of two-parameter eigenvalue problems, J. Comput. Appl. Math. 15 (1986) 109–115.
[49] F. Tisseur, K. Meerbergen, The quadratic eigenvalue problem, SIAM Rev. 43 (2001) 235–286.
[50] C. Vermeersch, B. De Moor, Globally optimal least-squares ARMA model identification is an eigenvalue problem, IEEE Control Syst. Lett. 3 (2019) 1062–1067.
[51] C. Vermeersch, B. De Moor, A column space based approach to solve systems of multivariate polynomial equations, IFAC-PapersOnLine 54 (2021) 137–144. Part of special issue: 24th International Symposium on Mathematical Theory of Networks and Systems (MTNS).
[52] H. Volkmer, Multiparameter Eigenvalue Problems and Expansion Theorems, Lecture Notes in Mathematics, vol. 1356, Springer, Berlin, Germany, 1988.